Chapter 5

NUMERICAL SIMULATION OF WOVEN COMPOSITES USING FINITE ELEMENT METHOD

5.0 Introduction

Textile materials are known by the distinct hierarchy of structure viz. fibre, yarn and fabric and garment. Though a number of investigations have taken place on these materials and many theoretical models exist for different textile structure, a model representing textile composite structure is mínimum.

Analytical/numerical textile modeling techniques (using a small representative piece of material, called unit cell (UC), which repeats over and over) completely describing the whole fabric have been described in Chapter 2.

In this chapter, numerical simulation of the mechanical properties in terms of tensile strength has been done with help of the Finite Element Method (FEM). Finite Element Analysis (FEA) software mostly uses two dimensional elements with layer capabilities to simúlate fibre reinforced composite materials. These elements require average material properties of fibre and matrix material, such as average Young's modulus, shear modulus and Poisson's ratio. Experiments on the real material are used to obtain these required properties.

5.1 Fabric Composites and it's Properties

The analyzed material is a woven carbon fabric($(C_{12K}C_{6K})_p$ with a uniform number of warp and filling threads (Figure 5.1) used for textile polymer textile composite laminate (TPCL). An epoxy resin is used as matrix. The material dimensions and properties are shown in (Table 5.1). In order to simplify the problem, a linear Young's modulus behavior is chosen for the epoxy resin, although the stress-strain behavior of such a material is nonlinear in reality as described by Merlin et al., 2009 [136].

Table 5.1: Properties of the Analyzed Material

Material	Young Modulus	Poisson's ratio	Cross section	Tensile strength
	N/mm^2	-	mm^2	N/mm^2
Fibre	230000	0.3	0.115	3500
Resin	3000	0.3	-	80

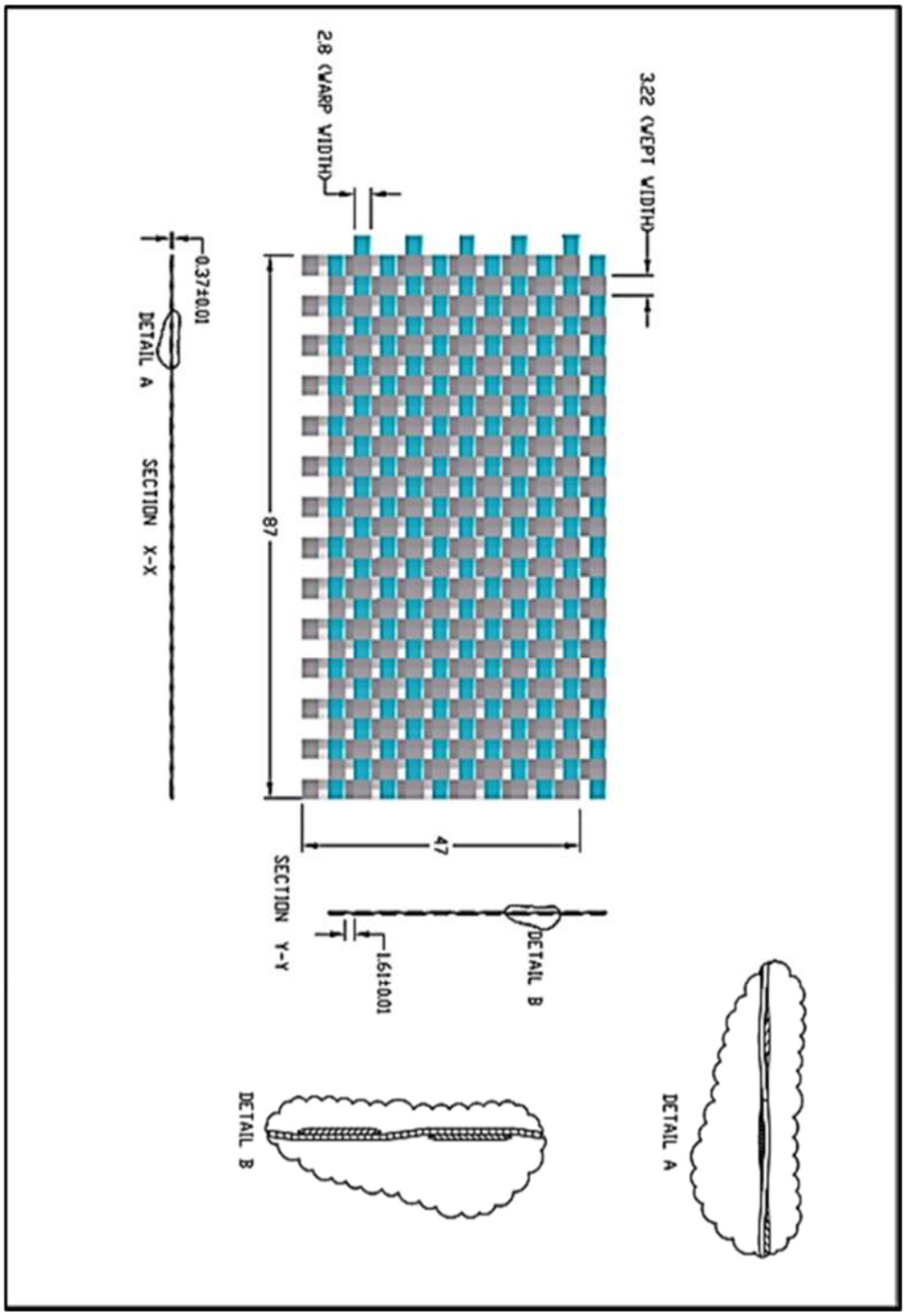

Figure 5.1: Detail of schematic diagram showing detail of CC1

The fabric composite (material), TPCL is as shown in Figure 5.2 is in three dimension and it is with different layers which includes five resin layers and four fabric layers.

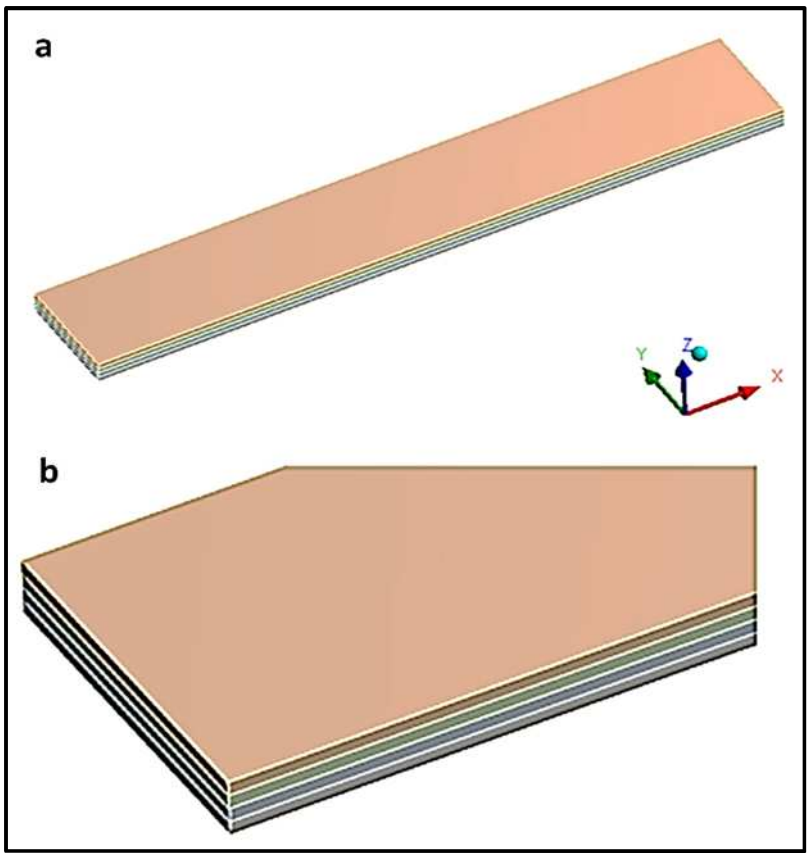

Figure 5.2: Diagram representing different fabric layers and resin layers.
(a- Fabric layers with resin layers; b- expanded view of a)

5.2 FEM Implementation

FEM application in textile composites can be visualized as assemblages of representative volume elements (RVEs) or unit cells, interconnected at discrete numbers of nodal points.

5.2.1 Mesh Formation

Now, discretization of the domain into finite elements using software Solid works. Here, the finite element has been considered as rectangular elements. Composite laminate (Figure 5.3 a) with rectangular mesh is shown in Figure 5.3 (b).

Figure 5.4 shows dialog box in software representing the number of nodes and number of elements. This material is discretized in to 76800 hexahedral elements as shown in Figure 5.4. Hence, this structure has 343297 nodes**.**

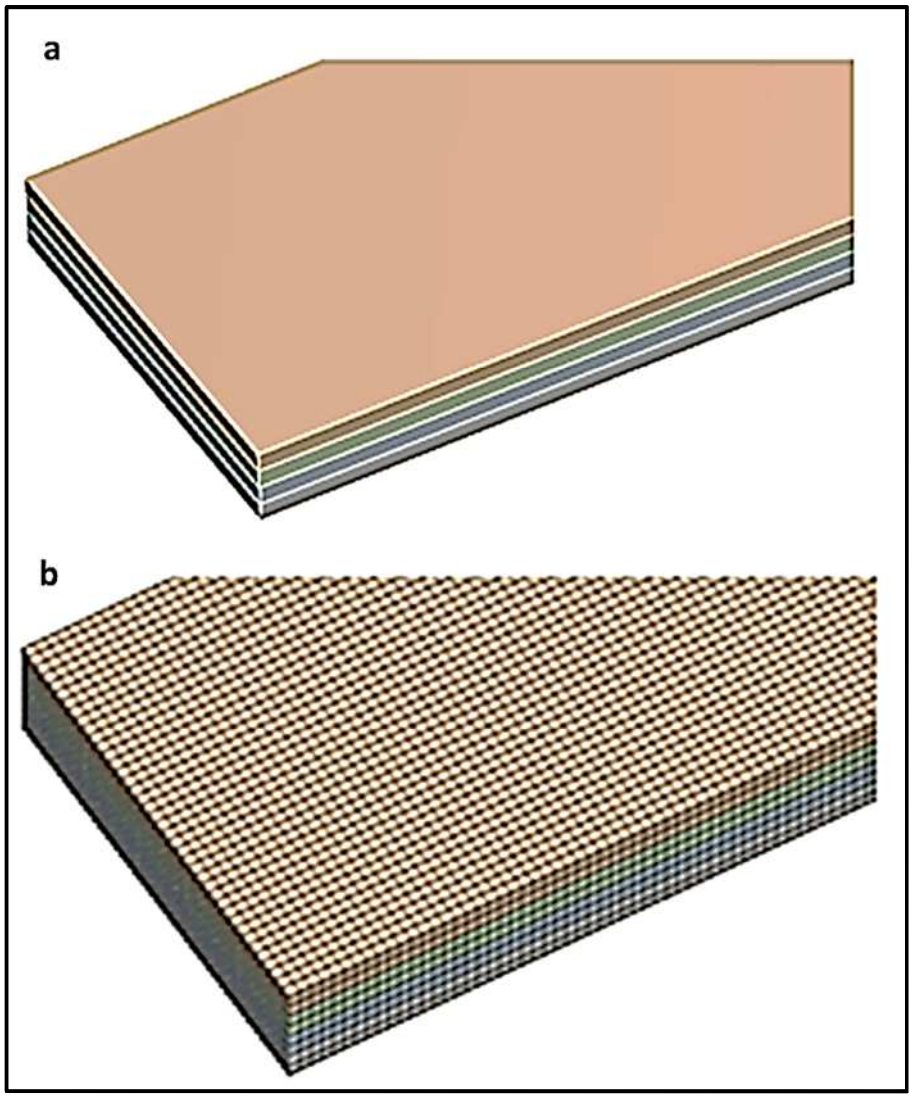

Figure 5.3: Diagram representing different fabric layers and resin layers with mesh formation.
(a- expanded view of Composite; b- composite with rectangular mesh)

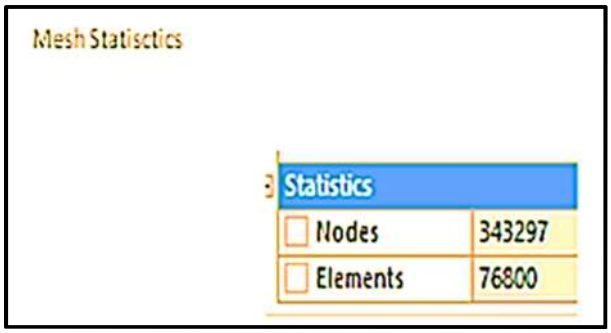

Figure 5.4: Dialog box representing the number of nodes and elements.

5.2.2 Stiffness Matrix and System of Equations

The geometry generated by Solid Works is initially saved in (.prt) file format which in turn exported in ANSYS/FLUENT environment.

Further the generation of material definition and boundary conditions are incorporated by certain operations. Here, force value has been given as loading condition. The boundary condition is the nodal displacement in the axial direction. That is, nodal displacement in axial direction is free (in Ansys software there are two pre-defined conditions, one is fixed and other is free) Based on our problem definition, it has been given free boundary conditions. The automated modeling approach with implicit FE scheme was carried for static simulations in the present investigation. (The details of FE modeling approach can be seen as in Chapter 2)

Equations for each element have been developed. After applying boundary conditions, initial conditions and loading, the global stiffness matrix has been constructed. Therefore, at every node it becomes the system of equations as shown in equation

$$Kd = f \qquad (5.1)$$

Where,

K is stiffness matrix,

d is displacement vector (deformation vector),

f is force

K is a matrix 343297x343297

d is a matrix 343297x 1

f is a matrix 343297x1

Later on, a set of linear or nonlinear algebraic equations have been solved simultaneously to obtain nodal displacement results. Using displacements, the strain value was found. Using Poison's ratio in Ansys stress had been evaluated.

5.3 Results and Discussion

In this work, the textile polymer composite laminates using 12K Carbon as warp and 6K Carbon as weft were prepared at different skew angles. These composites were used for the analysis and modeling. These composites were tested in both, longitudinal and transverse directions. Therefore, result and discussion are divided into two sections namely:

I) Longitudinal direction
II) Transverse direction.

For the understanding of phenomenon, the Carbon-Carbon composites were taken in all the five layering sequences as follows:

1. CC1 (0/0/0/0)
2. CC3 (0/+30/-30/0)
3. CC2 (0/+45/-45/0)
4. CC3 (0/+60/-60/0)
5. CC4 (0/+90/-90/0)

The details about the stacking sequence of Carbon- Carbon textile polymer composite laminates (TPCL) mentioned above are depicted in Table 3.3.

5.3.1 Longitudinal Results

In Figure 5.5a, deformation (2.25 mm) is observed in longitudinal simulation by considering all layers at 0/0/0/0 position. In Figure 5.5b, stress value (206.05 Mpa) is observed in longitudinal simulation by considering all layers at 0/0/0/0 position.

In Figure 5.6a, deformation (1.85 mm) is observed in longitudinal simulation by considering all layers at 0/+30/-30/0 position. In Figure 5.6b, stress value (261.58 Mpa) is observed as per shown above in longitudinal simulation by considering all layers at 0/+30/-30/0 position.

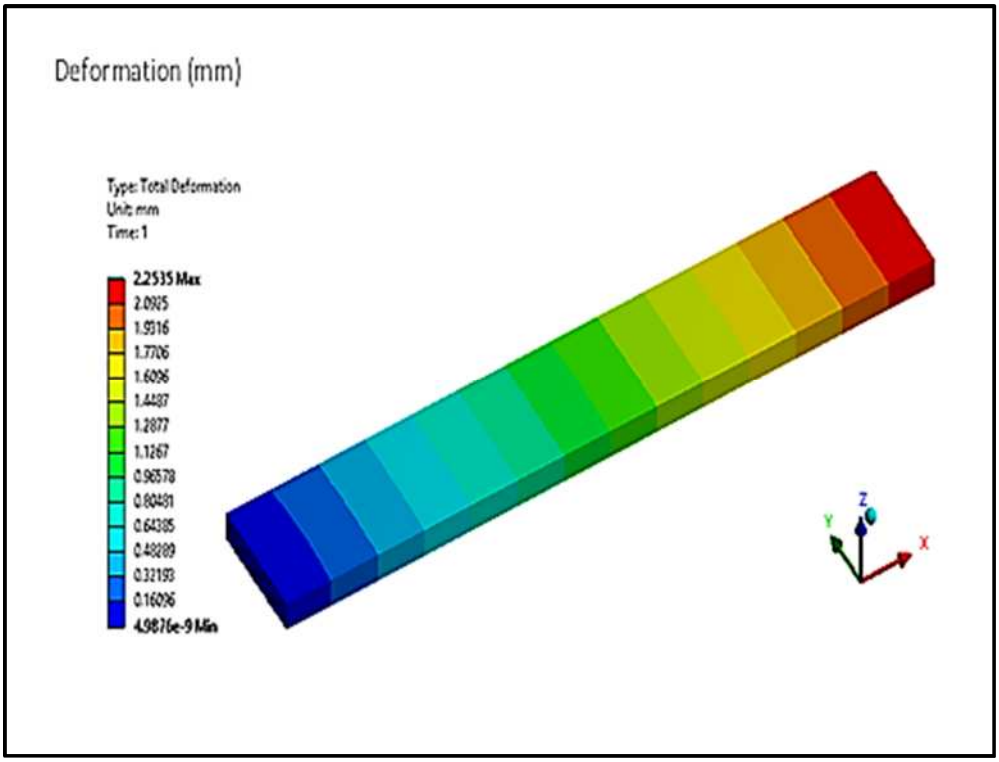

Figure 5.5a: Deformation of CC1 in longitudinal direction

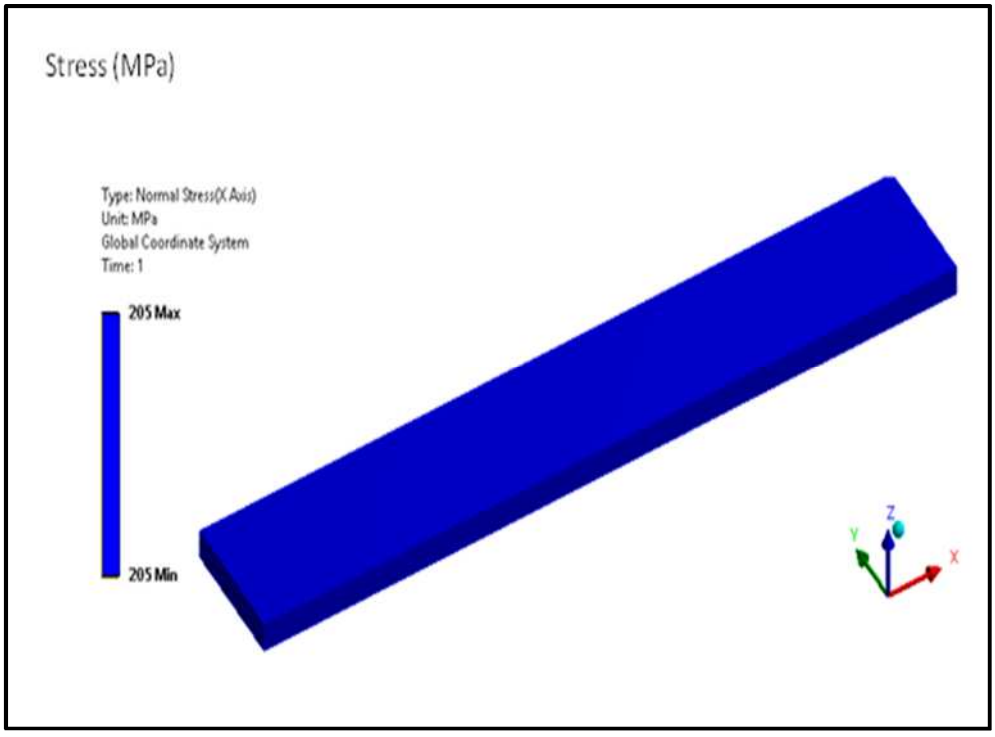

Figure 5.5b: Stress of CC1 in longitudinal direction

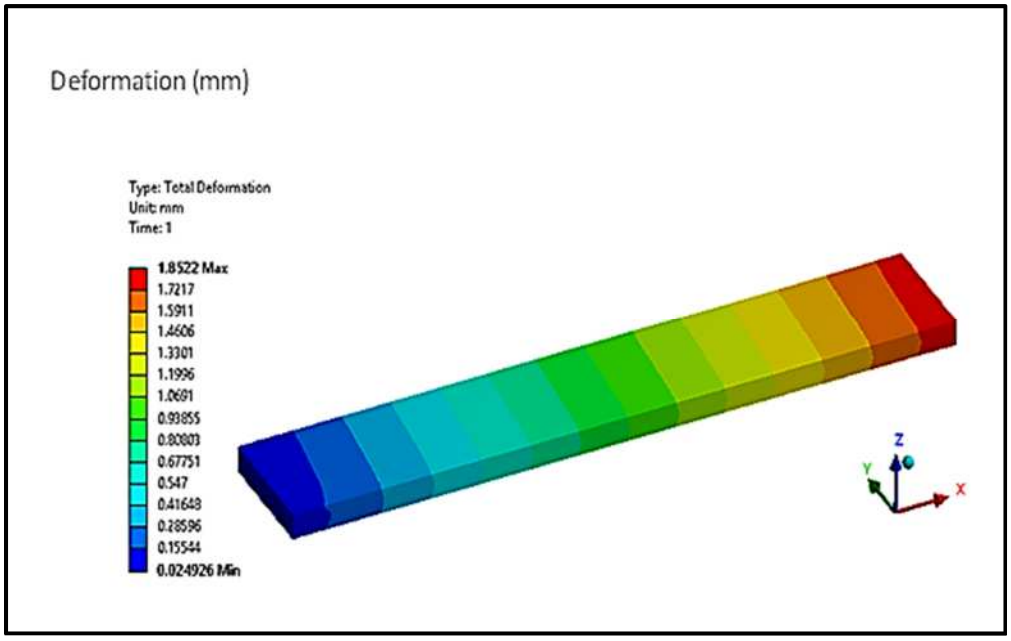

Figure 5.6a: Strain distribution of CC2 in longitudinal direction

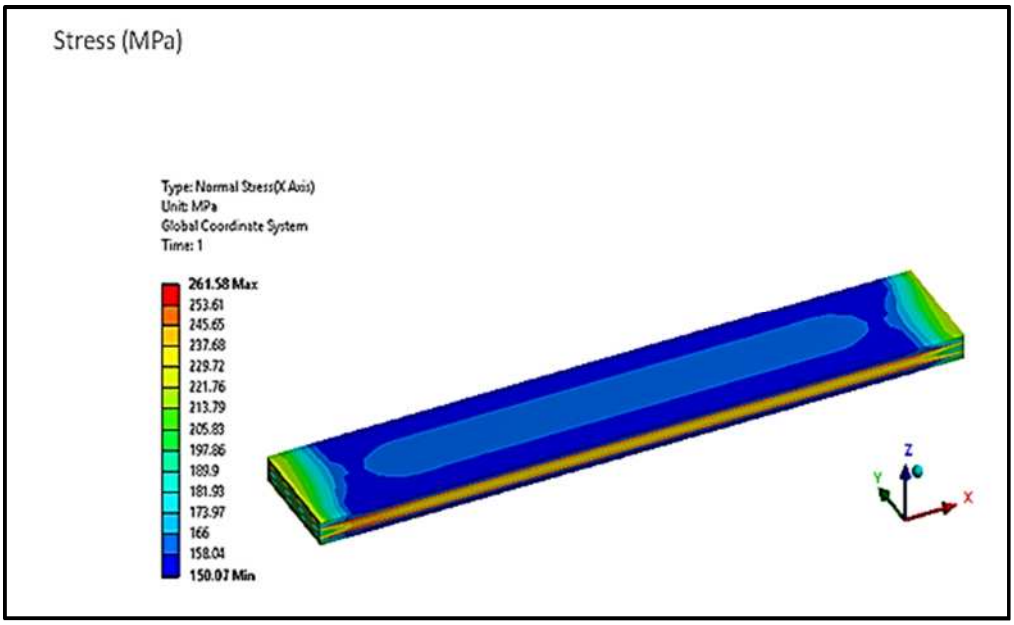

Figure 5.6b: Stress distribution of CC2 in longitudinal direction

In Figure 5.6c, stress 160.17 MPa is observed as per shown above in longitudinal simulation on 1st layer by considering all layers at 0/+30/-30/0 position. In Figure 5.6d, stress 250.93Mpa is observed as per shown above in longitudinal simulation on 2nd layer by considering all layers at 0/+30/-30/0 position.

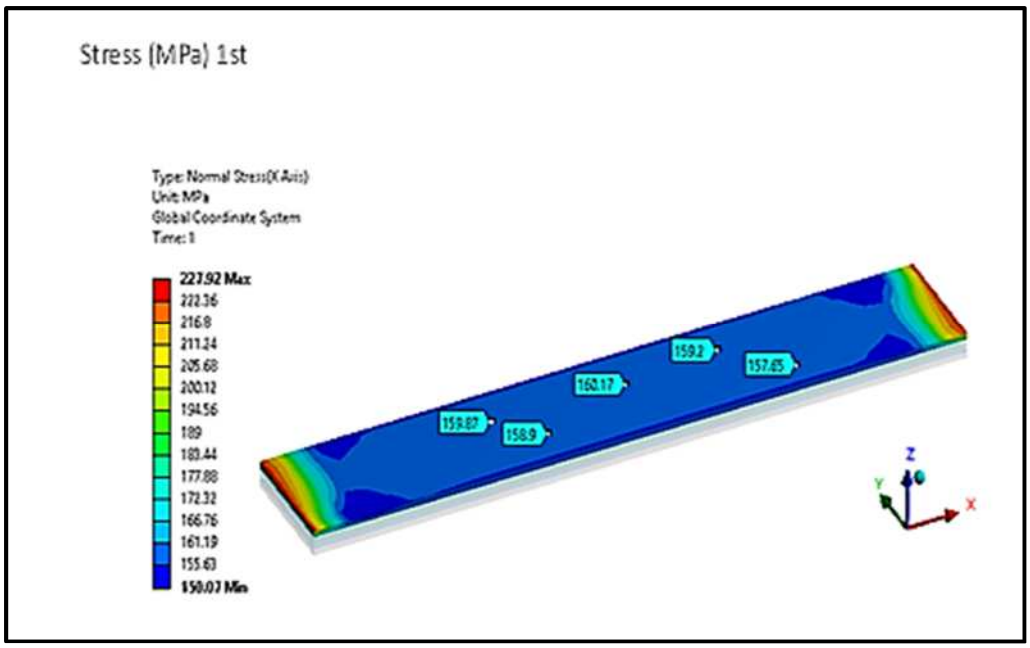

Figure 5.6c: Stress distribution of CC2 in longitudinal direction on the first layer

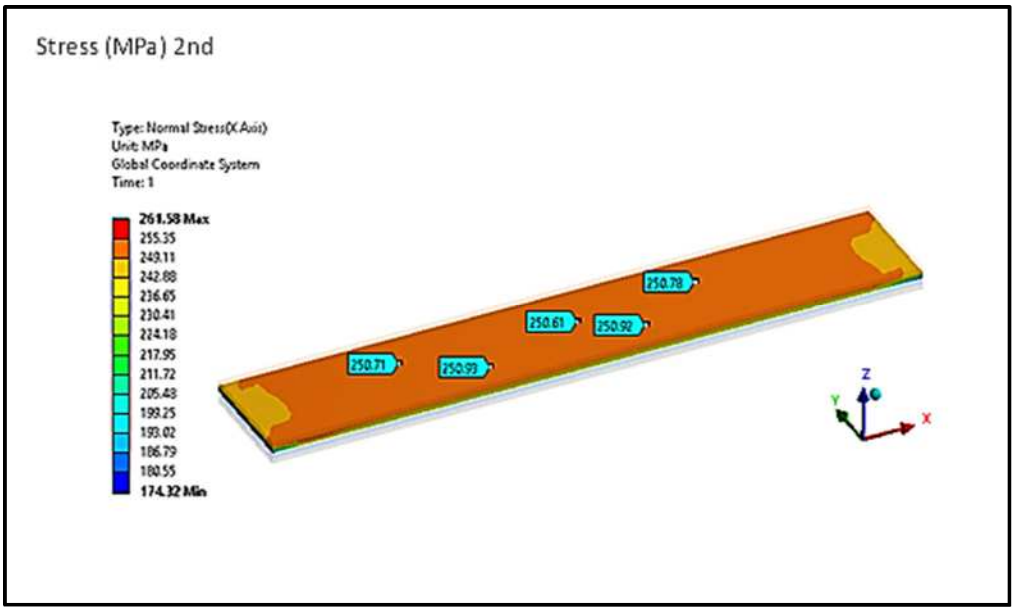

Figure 5.6d: Stress distribution of CC2 in longitudinal direction on the second layer

In Figure 5.6e, stress 251.86 Mpa is observed as per shown above in longitudinal simulation on 3rd layer by considering all layers at 0/+30/-30/0 position. In Figure 5.6f, stress 161.14 MPa is observed as per shown above in longitudinal simulation on 4th layer by considering all layers at 0/+30/-30/0 position.

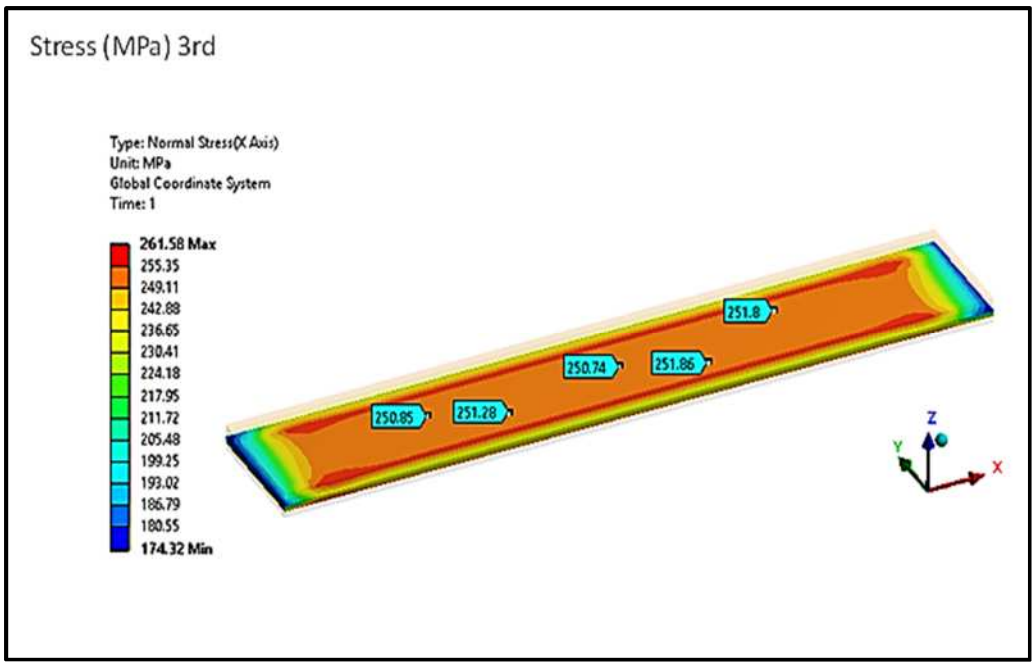

Figure 5.6e: Stress distribution of CC2 in longitudinal direction on the third layer

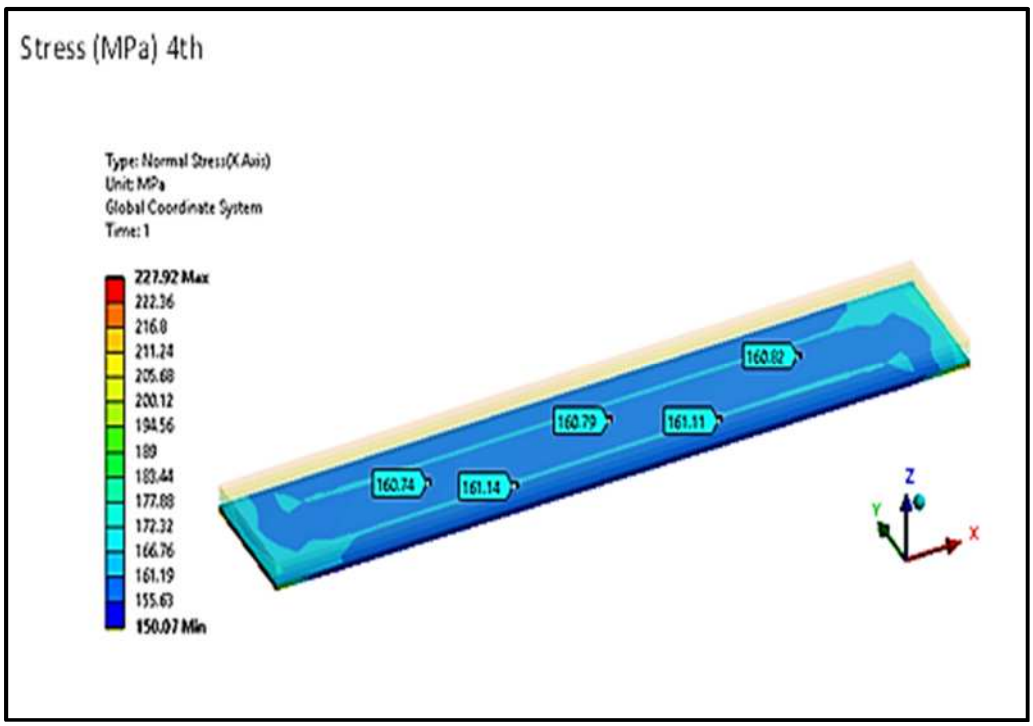

Figure 5.6f: Stress distribution of CC2 in longitudinal direction on the fourth layer

In Figure 5.7a, deformation 1.5134 mm is observed in longitudinal simulation by considering all layers at 0/+45/-45/0 position. In Figure 5.7b, Stress value

291.92 is observed as per shown above in longitudinal simulation by considering all layers at 0/+45/-45/0 position.

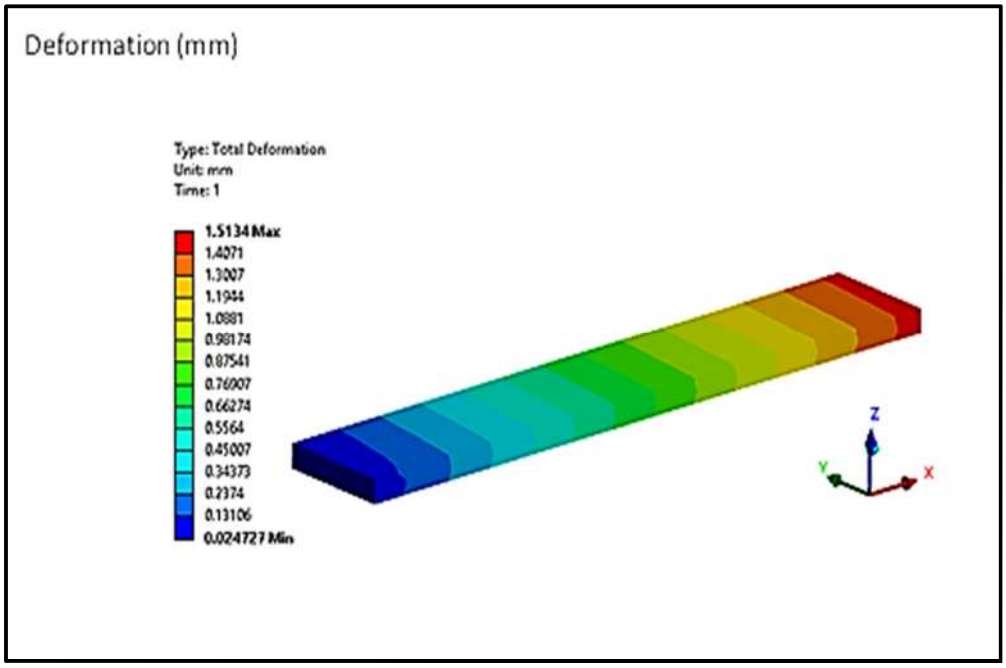

Figure 5.7a: Strain distribution of CC3 in longitudinal direction

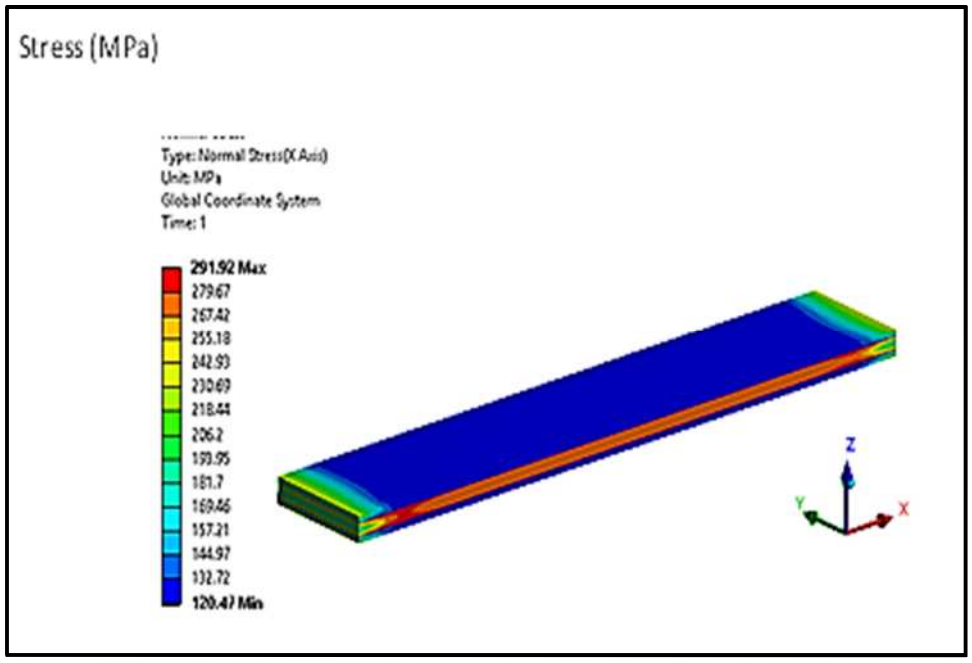

Figure 5.7b: Stress distribution of CC3 in longitudinal direction

In Figure 5.7c, stress 129.64 MPa is observed as per shown above in longitudinal simulation on 1st layer by considering all layers at 0/+45/-45/0

position. In Figure 5.7d, stress 281.33 Mpa is observed as per shown above in longitudinal simulation on 2nd layer by considering all layers at 0/+45/-45/0 position.

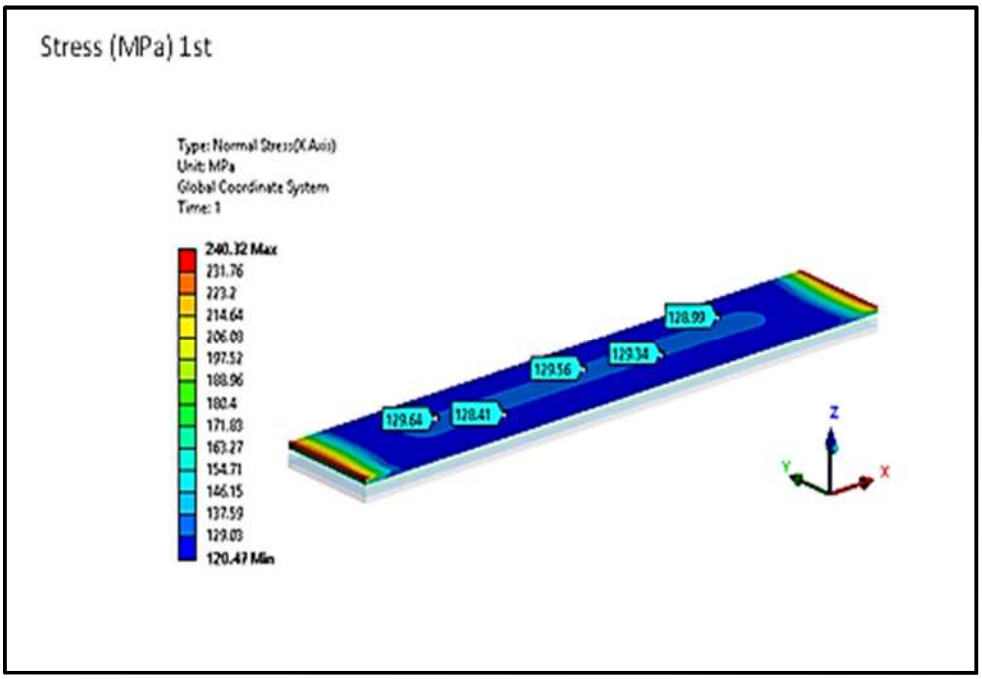

Figure 5.7c: Stress distribution of CC3 in longitudinal direction on the first layer

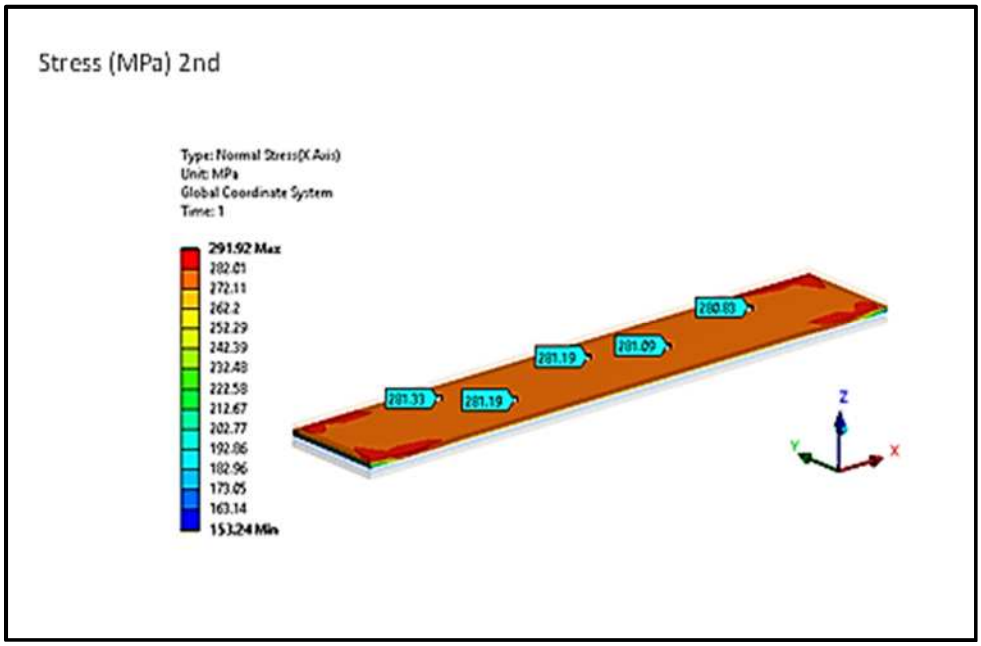

Figure 5.7d: Stress distribution of CC3 in longitudinal direction on the second layer

In Figure 5.7e, stress 281.44 MPa is observed as per shown above in longitudinal simulation on 3rd layer by considering all layers at 0/+45/-45/0 position. In Figure 5.7f, stress 129.85 MPa is observed as per shown above in longitudinal simulation on 4th layer by considering all layers at 0/+45/-45/0 position.

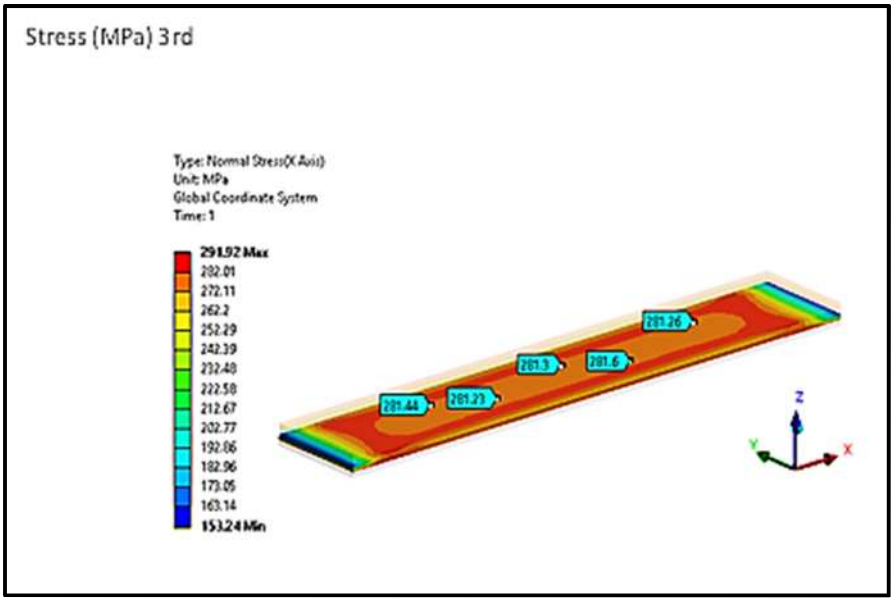

Figure 5.7e: Stress distribution of CC3 in longitudinal direction on the third layer

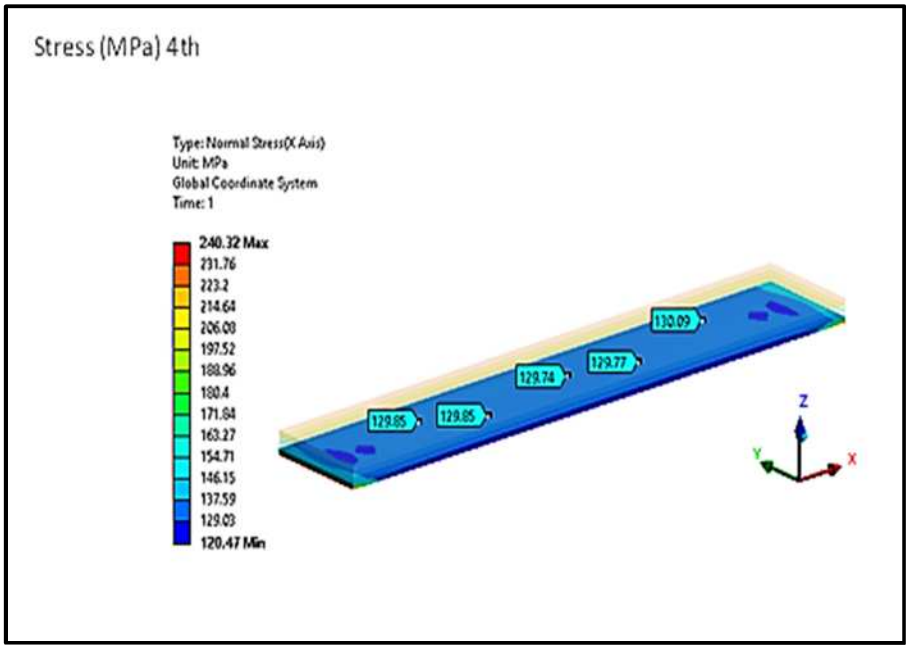

Figure 5.7f: Stress distribution of CC3 in longitudinal direction on the fourth layer

In Figure 5.8a, deformation 1.3098 mm is observed in longitudinal simulation by considering all layers at 0/+60/-60/0 position. In Figure 5.8b, stress behavior is observed as per shown above in longitudinal simulation by considering all layers at 0/+60/-60/0 position.

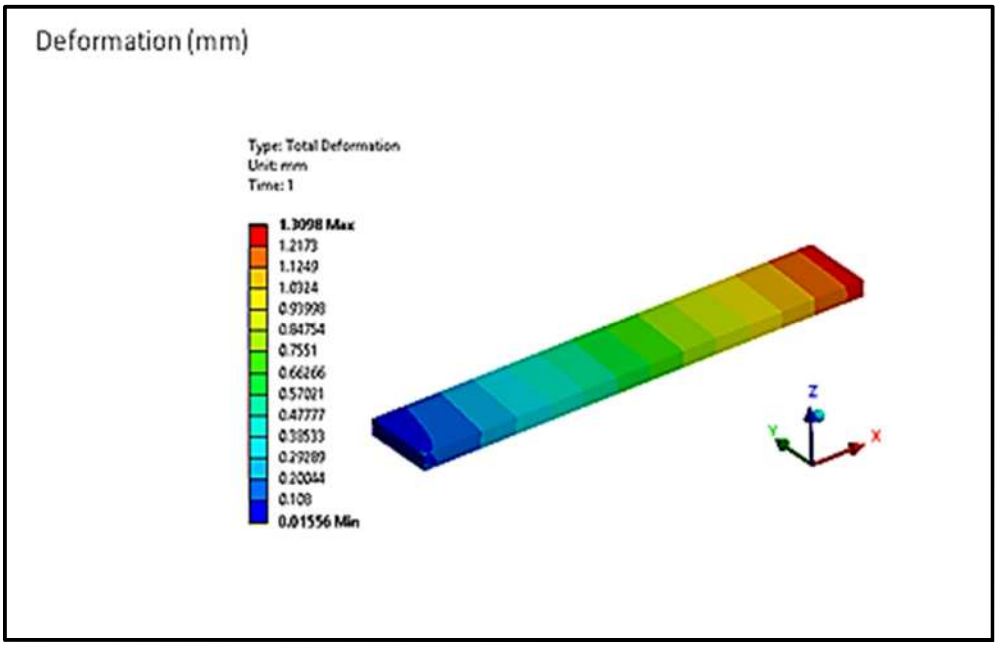

Figure 5.8a: Strain distribution of CC4 in longitudinal direction

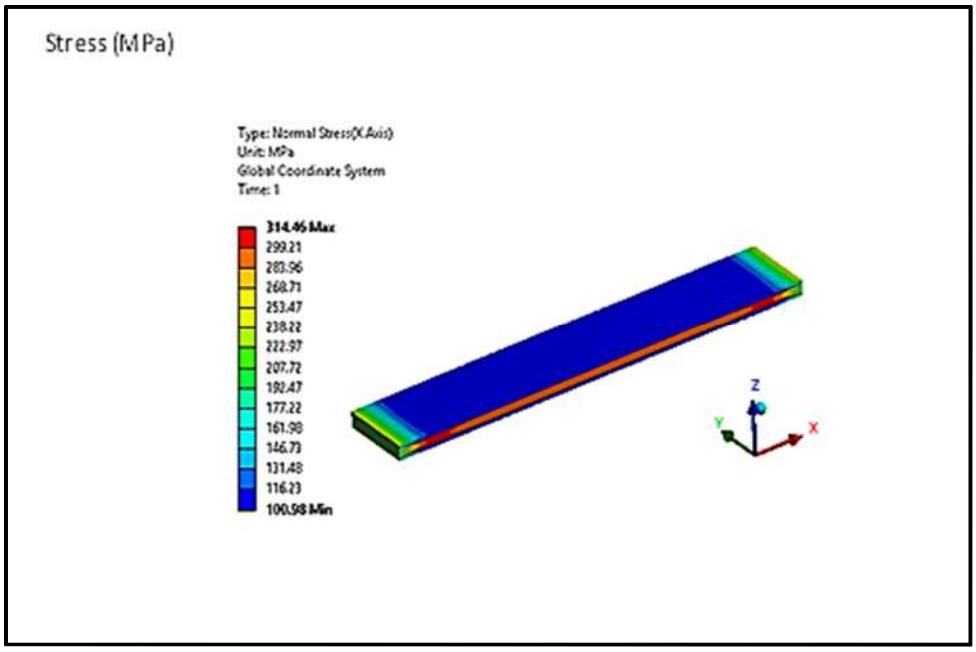

Figure 5.8b: Stress distribution of CC4 in longitudinal direction

In Figure 5.8c, stress 109.95 MPa is observed as per shown above in longitudinal simulation on 1st layer by considering all layers at 0/+60/-60/0 position. In Figure 5.8d, stress 302.32 Mpa is observed as per shown above in longitudinal simulation on 2nd layer by considering all layers at 0/+60/-60/0 position.

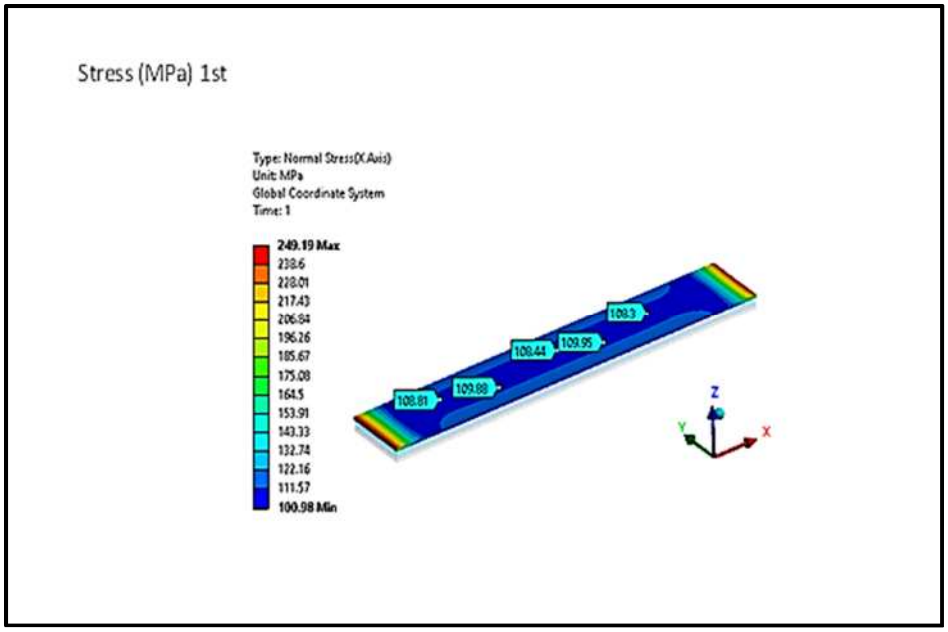

Figure 5.8c: Stress distribution of CC4 in longitudinal direction on the first layer

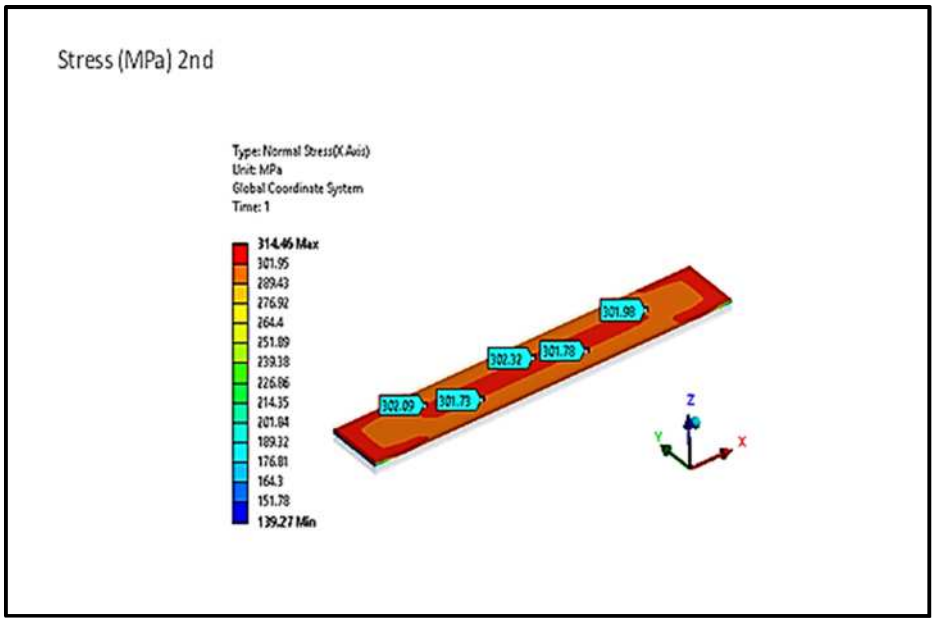

Figure 5.8d: Stress distribution of CC4 in longitudinal direction on the second layer

In Figure 5.8e, stress 301.62 Mpa is observed as per shown above in longitudinal simulation on 3rd layer by considering all layers at 0/+60/-60/0 position. In Figure 5.8f, stress 107.85 MPa is observed as per shown above in longitudinal simulation on 4th layer by considering all layers at 0/+60/-60/0 position.

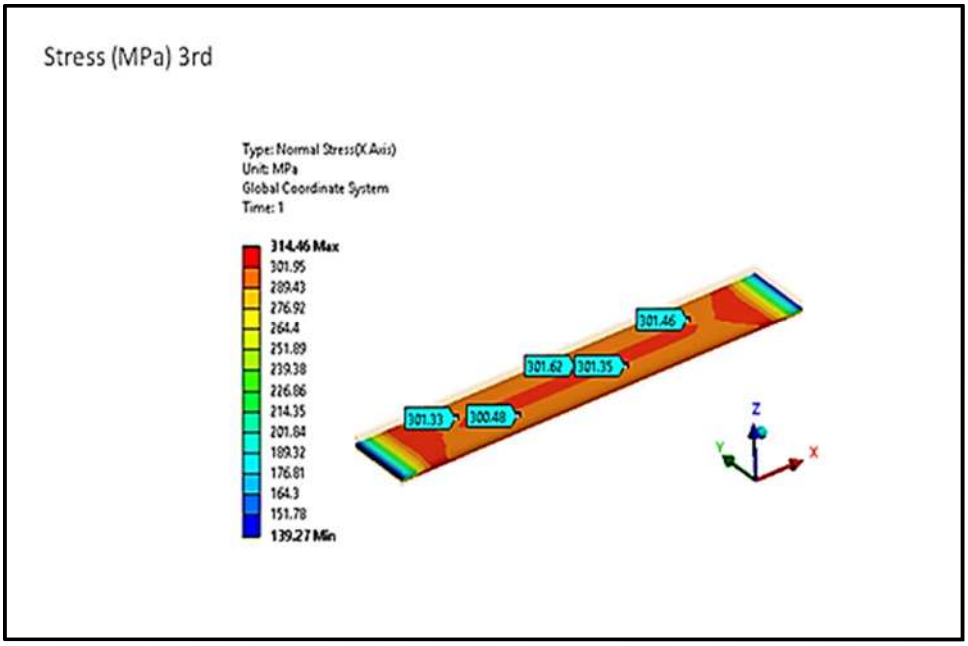

Figure 5.8e: Stress distribution of CC4 in longitudinal direction on the third layer

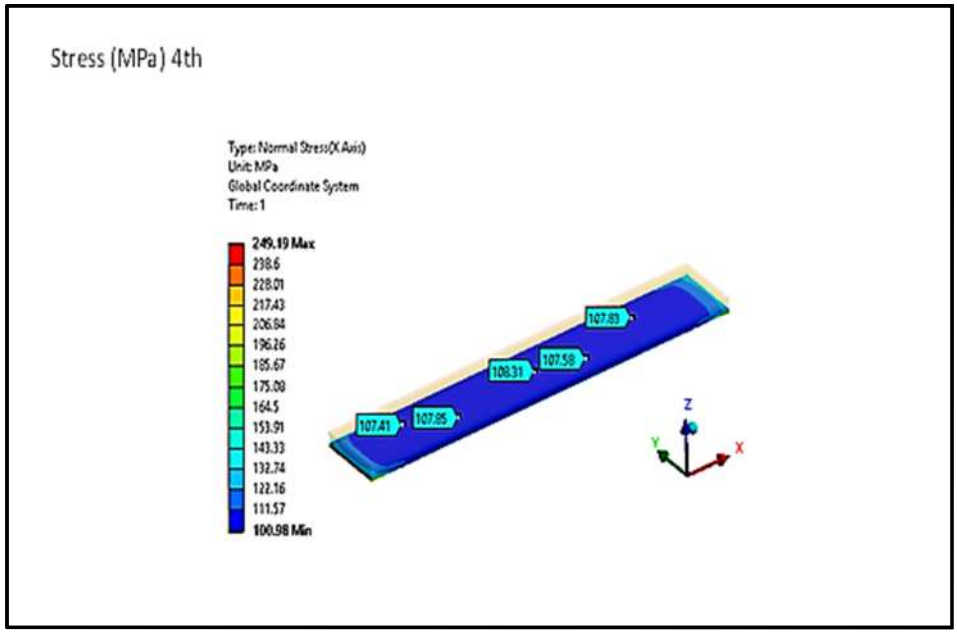

Figure 5.8f: Stress distribution of CC4 in longitudinal direction on the fourth layer

In Figure 5.9a, deformation 1.265 mm is observed in longitudinal simulation by considering all layers at 0/+90/-90/0 position. In Figure 5.9b, stress behavior is observed as per shown above in longitudinal simulation by considering all layers at 0/+90/-90/0 position.

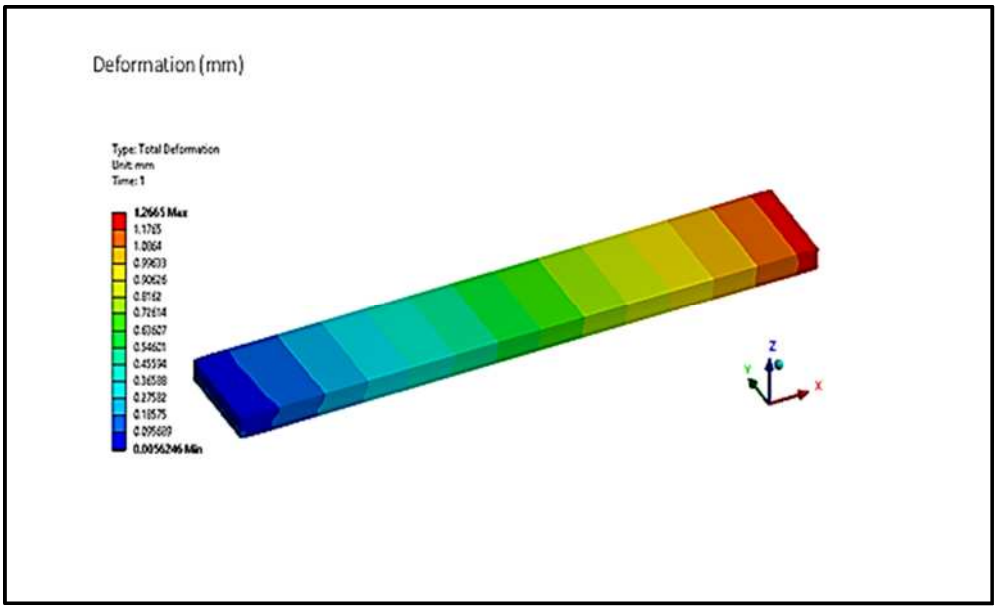

Figure 5.9a: Strain distribution of CC5 in longitudinal direction

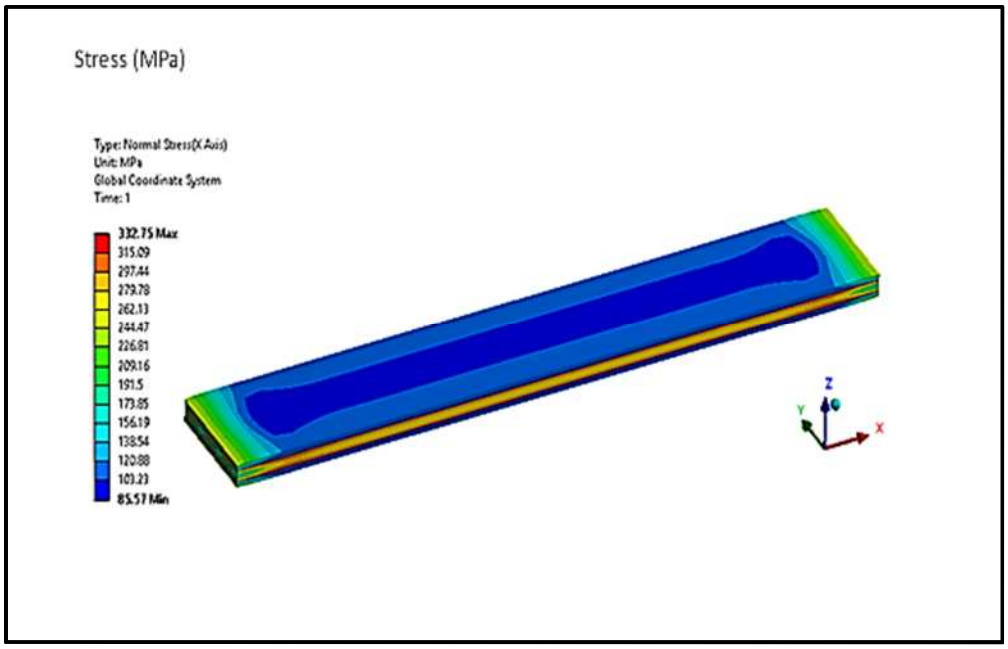

Figure 5.9b: Stress distribution of CC5 in longitudinal direction

In Figure 5.9c, stress 111.66 MPa is observed as per shown above in longitudinal simulation on 1st layer by considering all layers at 0/+90/-90/0

position. In Figure 5.9d, stress 322.81 Mpa is observed as per shown above in longitudinal simulation on 2nd layer by considering all layers at 0/+90/-90/0 position.

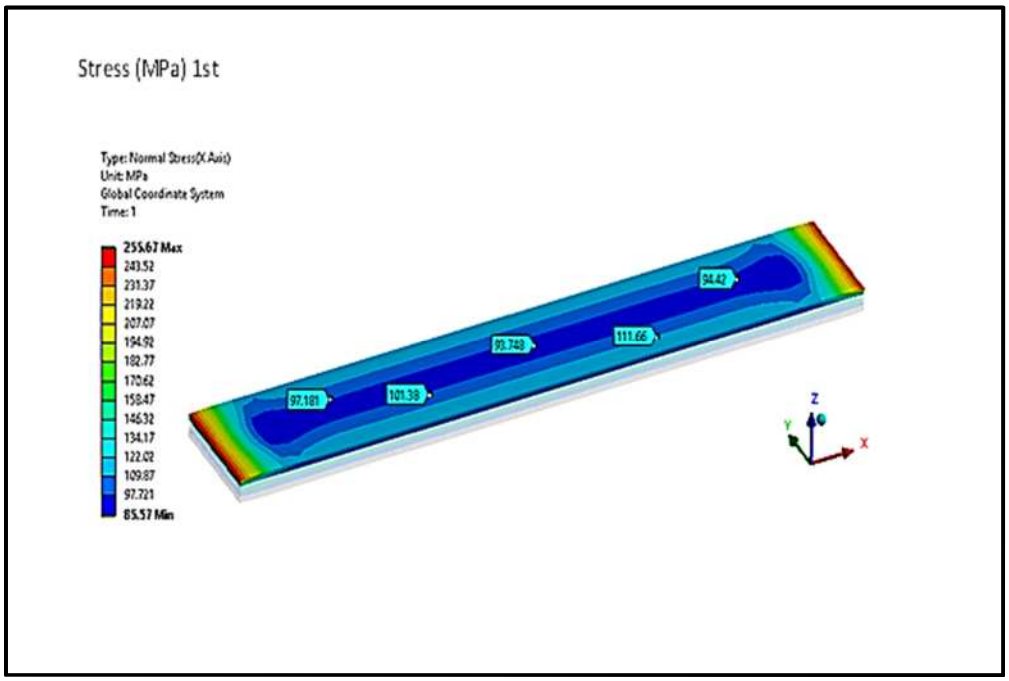

Figure 5.9c: Stress distribution of CC5 in longitudinal direction on the first layer

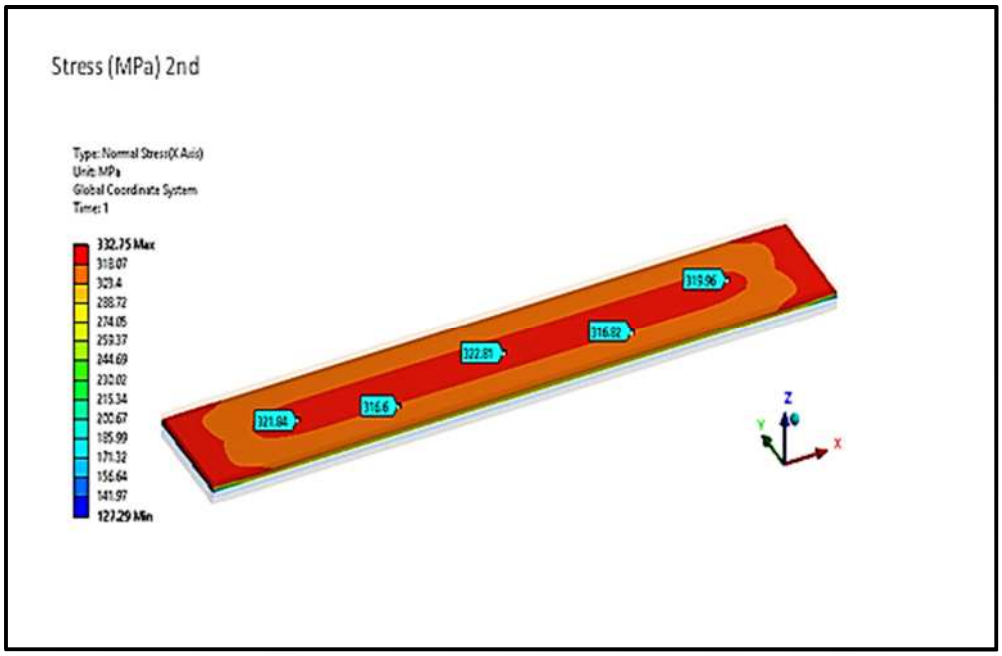

Figure 5.9d: Stress distribution of CC5 in longitudinal direction on the second layer

In Figure 5.9e, stress 322.54 Mpa is observed as per shown above in longitudinal simulation on 3rd layer by considering all layers at 0/+90/-90/0 position. In Figure 5.9f, stress 95.024 MPa is observed as per shown above in longitudinal simulation on 4th layer by considering all layers at 0/+90/-90/0 position.

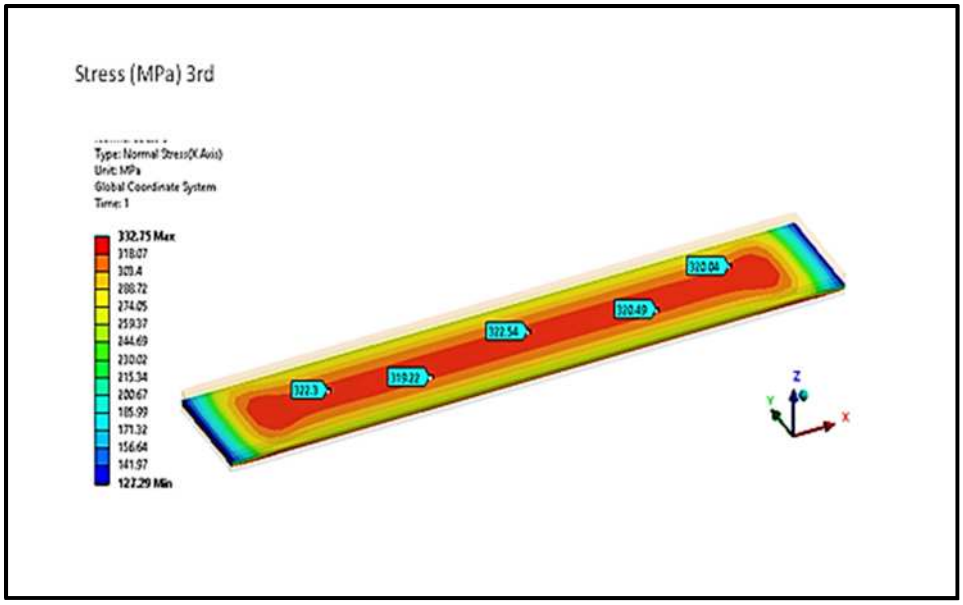

Figure 5.9e: Stress distribution of CC5 in longitudinal direction on the third layer

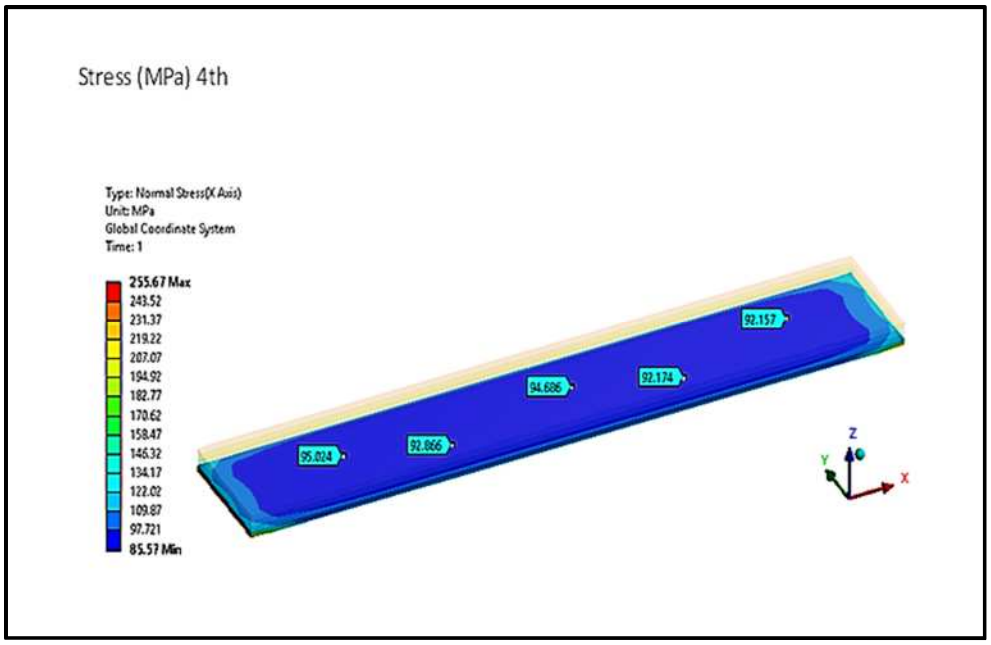

Figure 5.9f: Stress distribution of CC5 in longitudinal direction on the fourth layer

5.3.2 Transverse Results

In Figure 5.10a, deformation 0.871 mm is observed in transverse simulation by considering all layers at 0/0/0/0 position. In Figure 5.10b, stress 205 MPa is observed in Transverse simulation by considering all layers at 0/0/0/0 position.

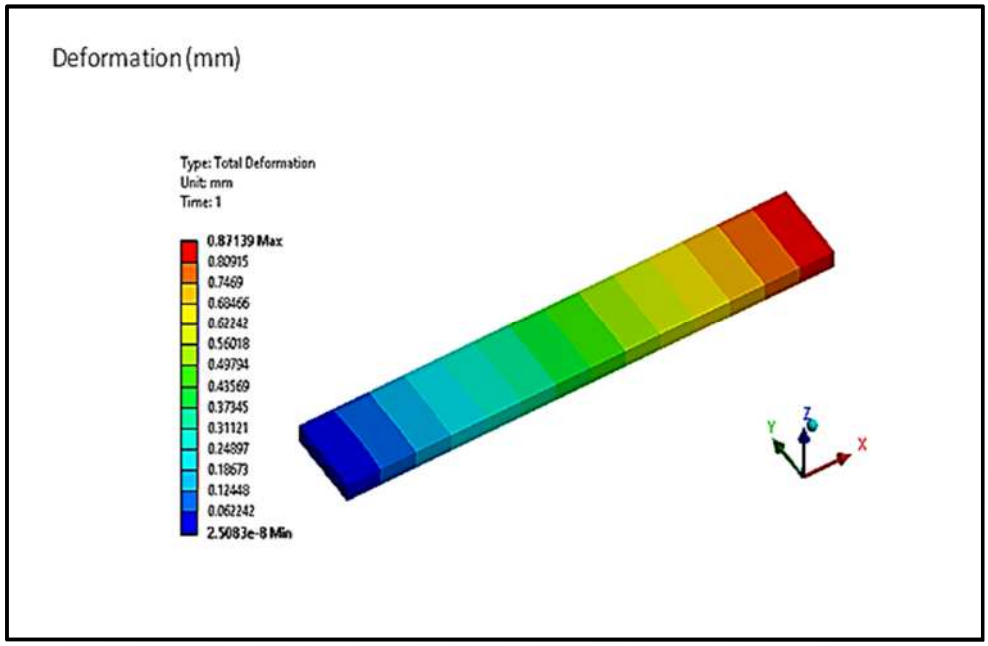

Figure 5.10a: Strain distribution of CC1 in transverse direction

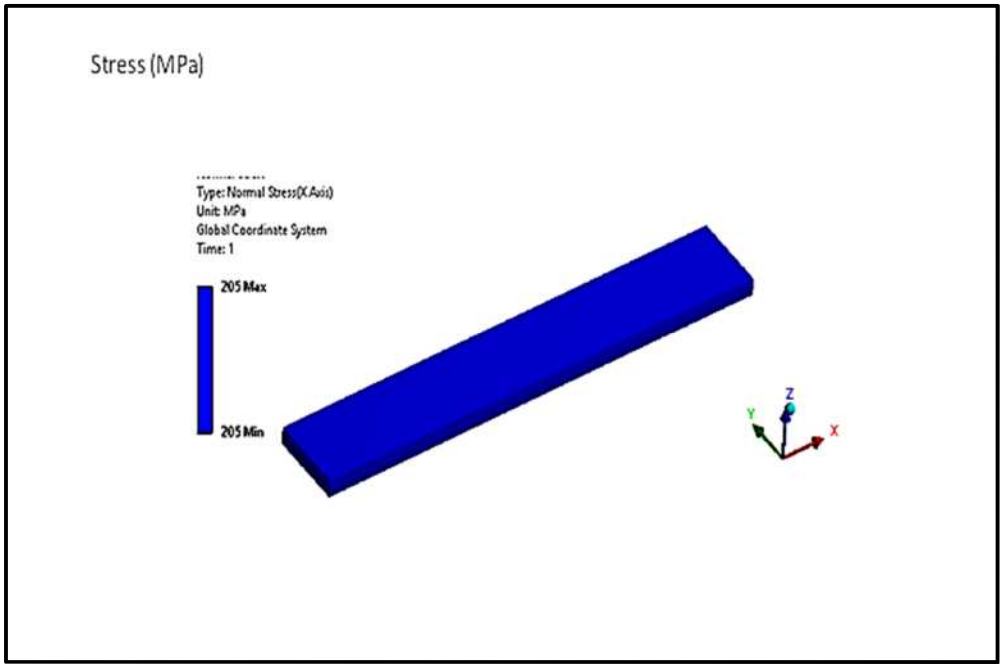

Figure 5.10b: Stress distribution of CC1 in transverse direction

In Figure 5.11a, deformation 0.94586 mm is observed in Transverse simulation by considering all layers at 0/+30/-30/0 position. In Figure 5.11b stress behavior is observed as per shown above in Transverse simulation by considering all layers at 0/+30/-30/0 position.

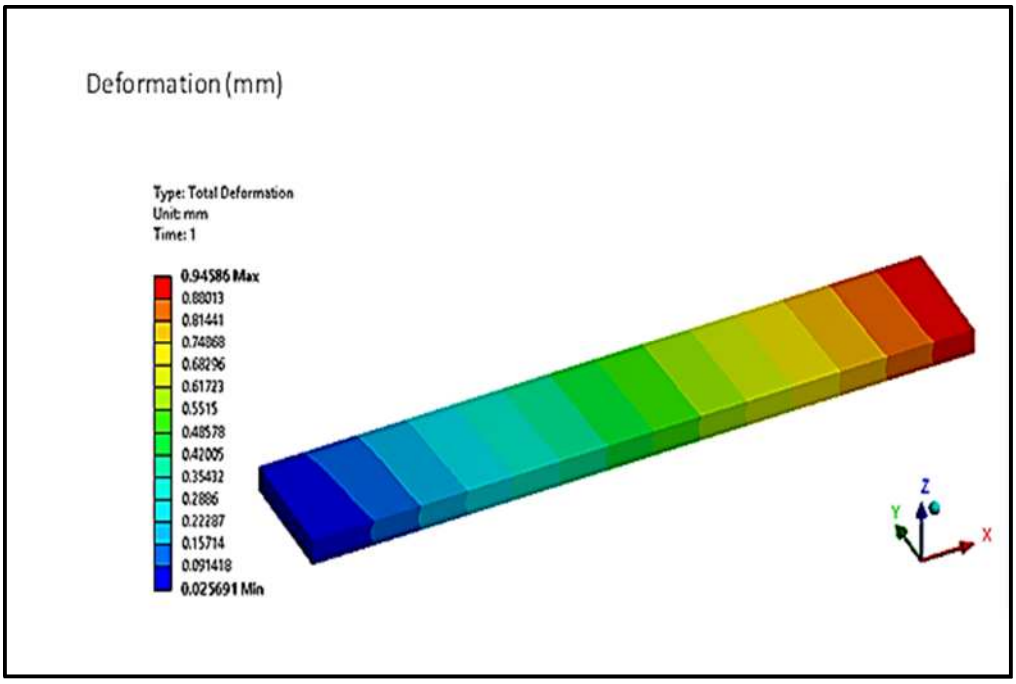

Figure 5.11a: Strain distribution of CC2 in transverse direction

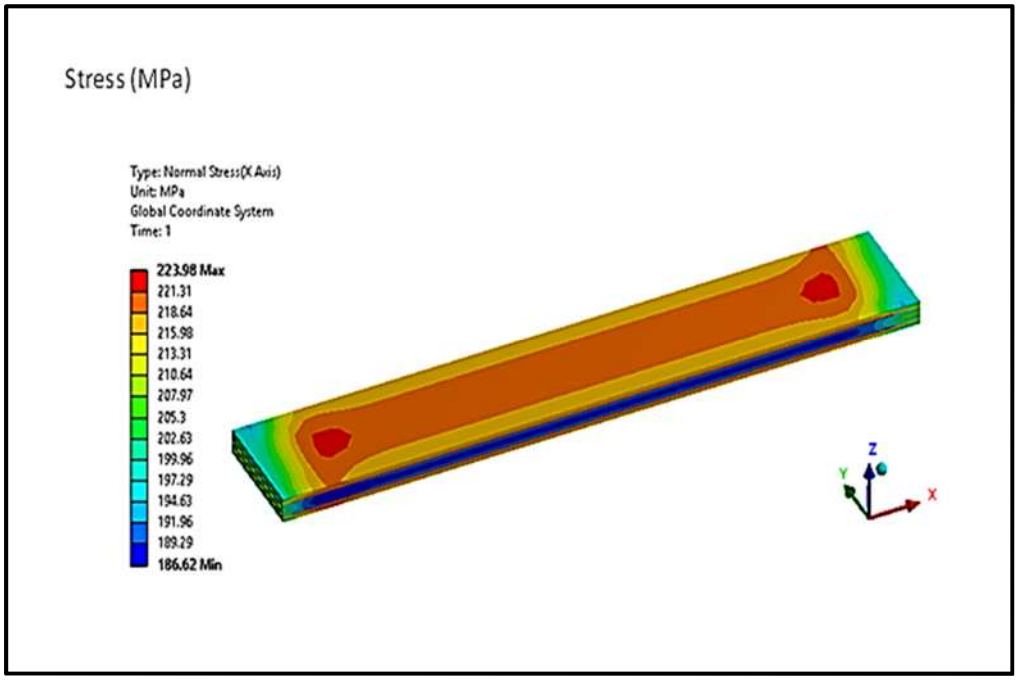

Figure 5.11b: Stress distribution of CC2 in transverse direction

In Figure 5.11c, stress 220.74 MPa is observed as per shown above in Transverse simulation on 1st layer by considering all layers at 0/+30/-30/0 position. In Figure 5.11d, stress 190.13 Mpa is observed as per shown above in Transverse simulation on 2nd layer by considering all layers at 0/+30/-30/0 position.

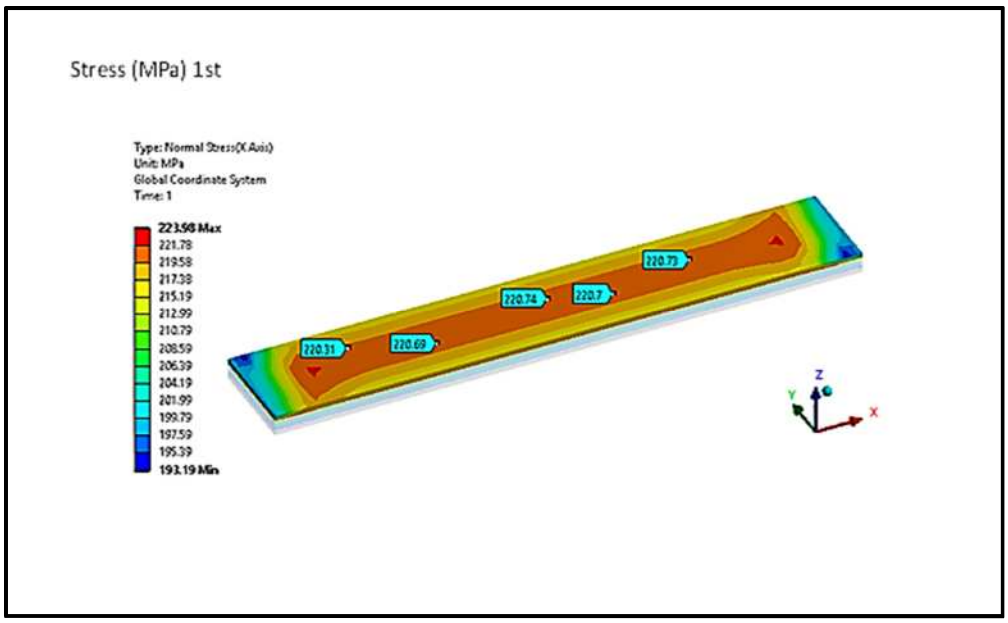

Figure 5.11c: Stress distribution of CC2 in transverse direction on the first layer

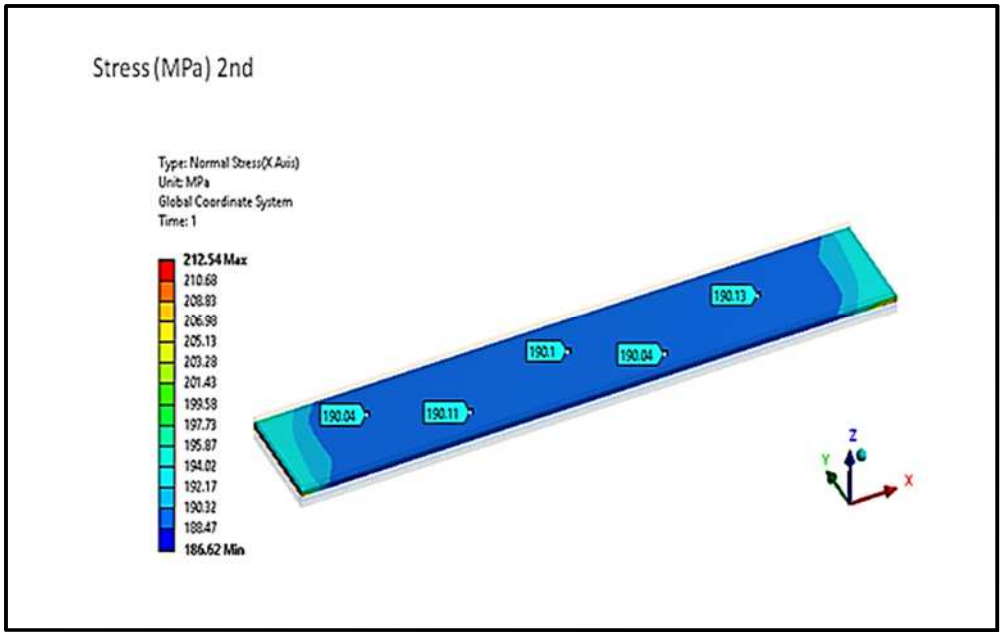

Figure 5.11d: Stress distribution of CC2 in transverse direction on the second layer

In Figure 5.11e, stress 190.11 Mpa is observed as per shown above in Transverse simulation on 3rd layer by considering all layers at 0/+30/-30/0 position. In Figure 5.11f, stress 229.52 MPa is observed as per shown above in Transverse simulation on 4th layer by considering all layers at 0/+30/-30/0 position.

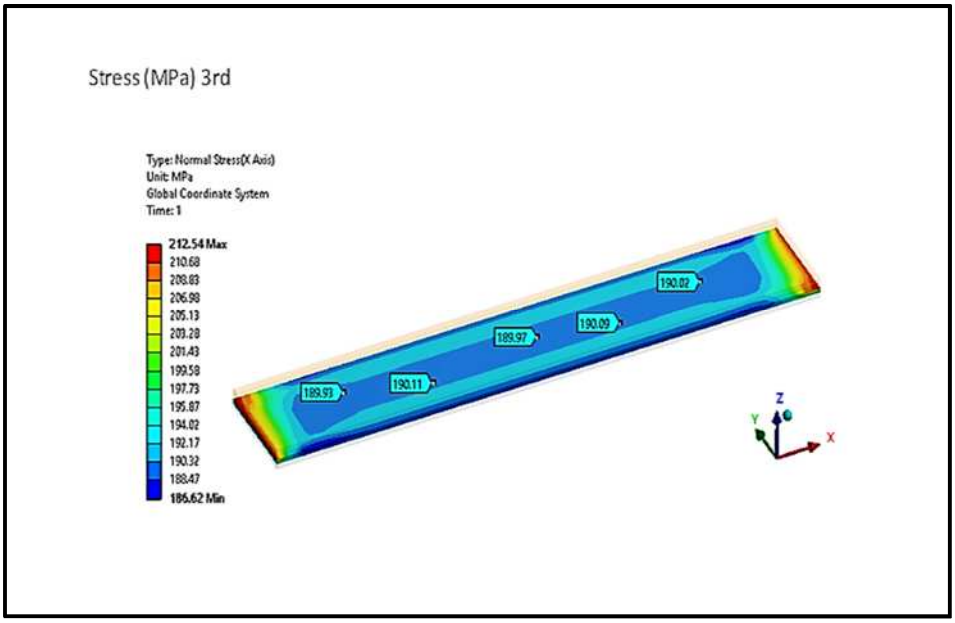

Figure 5.11e: Stress distribution of CC2 in transverse direction on the third layer

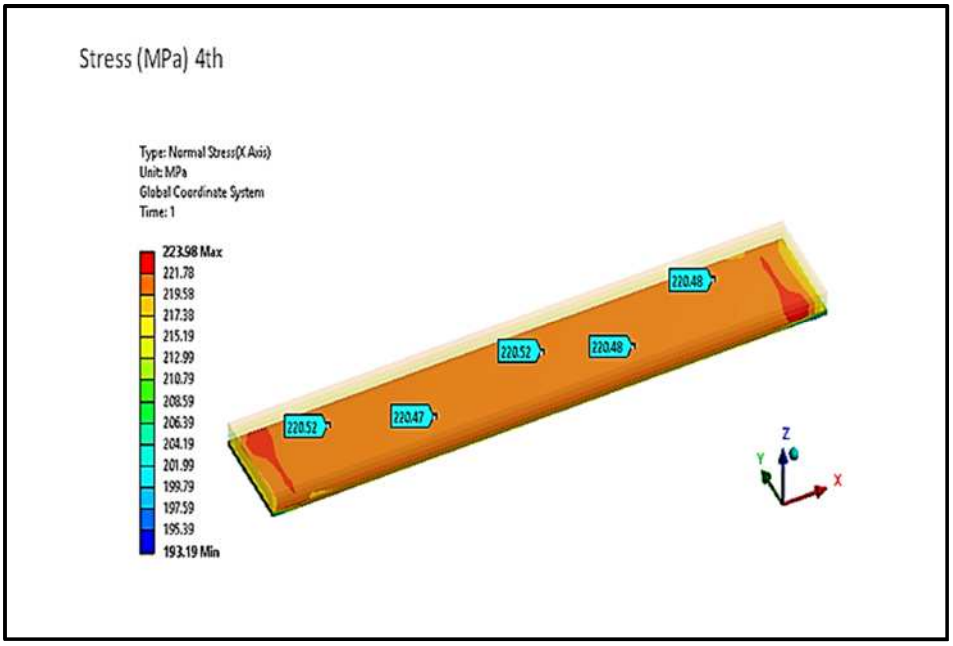

Figure 5.11f: Stress distribution of CC2 in transverse direction on the fourth layer

In Figure 5.12a, deformation 1.0577 mm is observed in Transverse simulation by considering all layers at 0/+45/-45/0 position. In Figure 5.12b, stress behavior is observed as per shown above in Transverse simulation by considering all layers at 0/+45/-45/0 position.

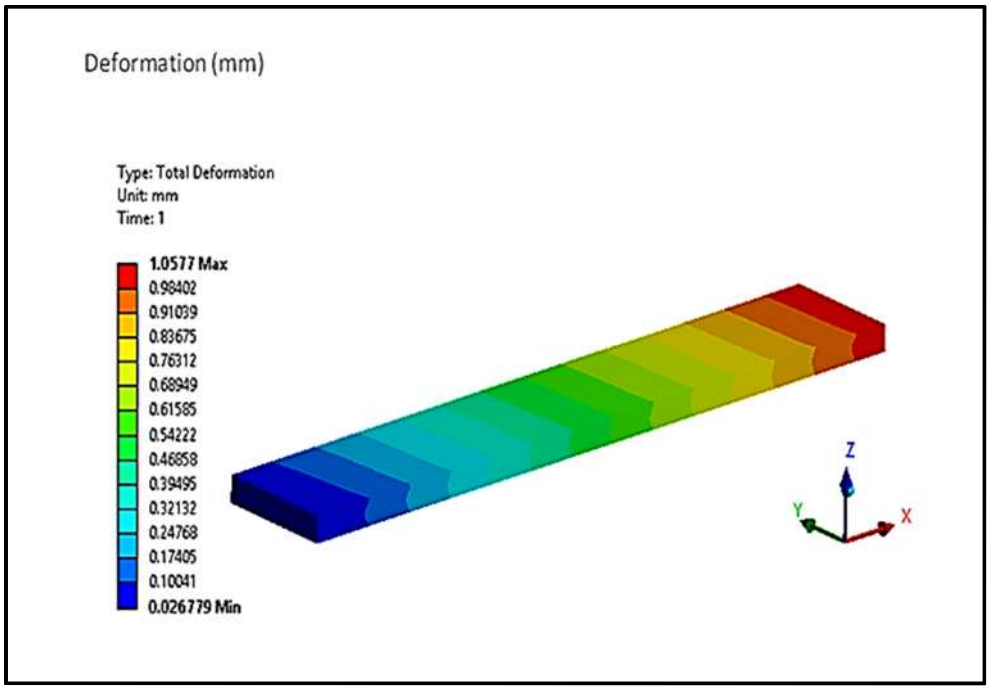

Figure 5.12a: Strain distribution of CC3 in transverse direction

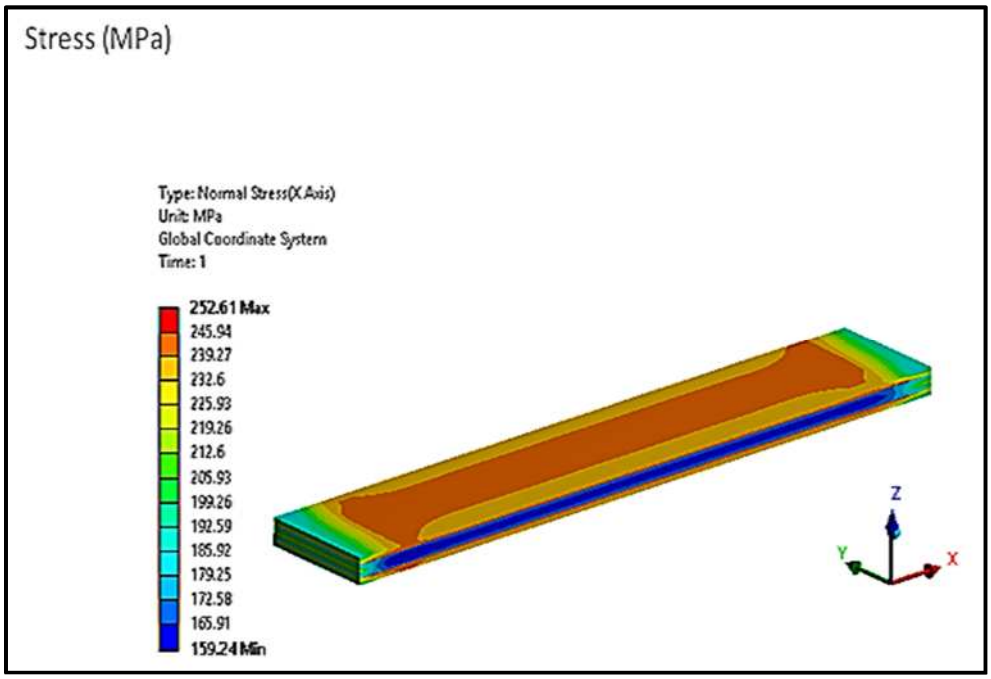

Figure 5.12b: Stress distribution of CC3 in transverse direction

In Figure 5.12c, stress 241.44 MPa is observed as per shown above in Transverse simulation on 1st layer by considering all layers at 0/+45/-45/0 position. In Figure 5.12d, stress 169.39 Mpa is observed as per shown above in Transverse simulation on 2nd layer by considering all layers at 0/+45/-45/0 position.

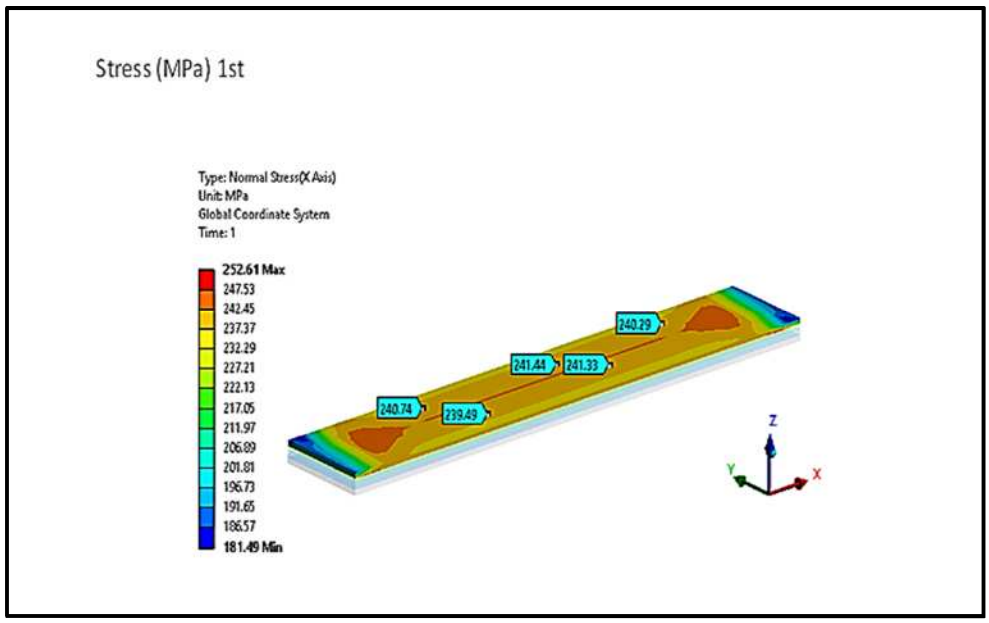

Figure 5.12c: Stress distribution of CC3 in transverse direction on the first layer

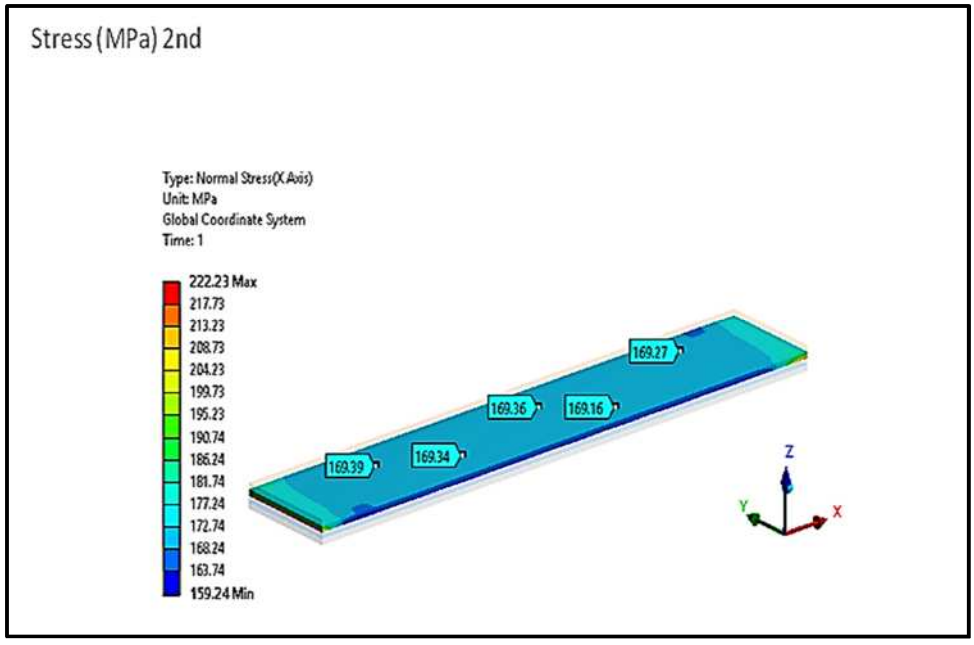

Figure 5.12d: Stress distribution of CC3 in transverse direction on the second layer

In Figure 5.12e, stress 169.58 MPa is observed as per shown above in Transverse simulation on 3rd layer by considering all layers at 0/+45/-45/0 position. In Figure 5.12f, stress 241.96 MPa is observed as per shown above in Transverse simulation on 4th layer by considering all layers at 0/+45/-45/0 position.

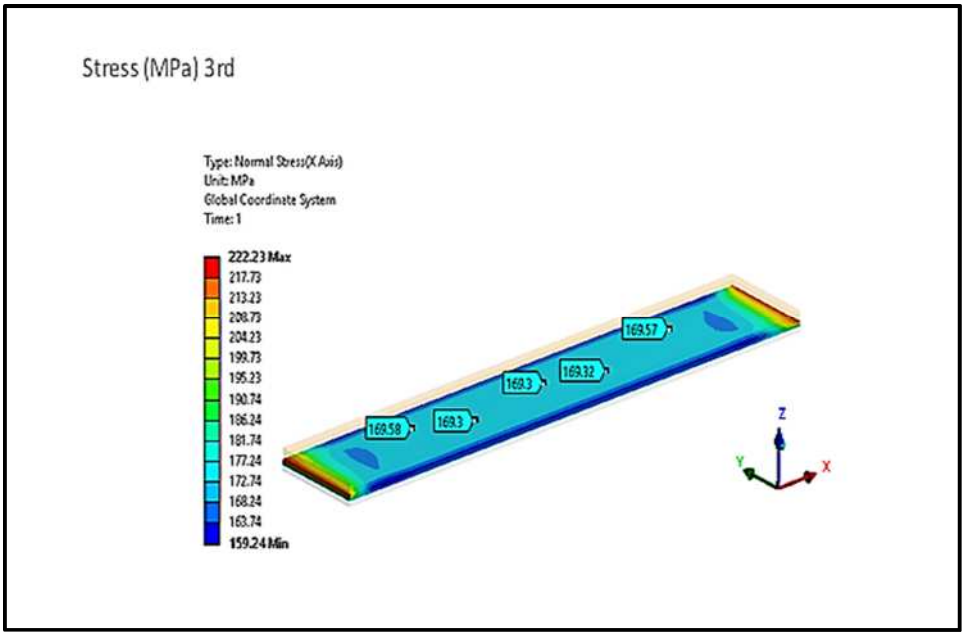

Figure 5.12e: Stress distribution of CC3 in transverse direction on the second layer

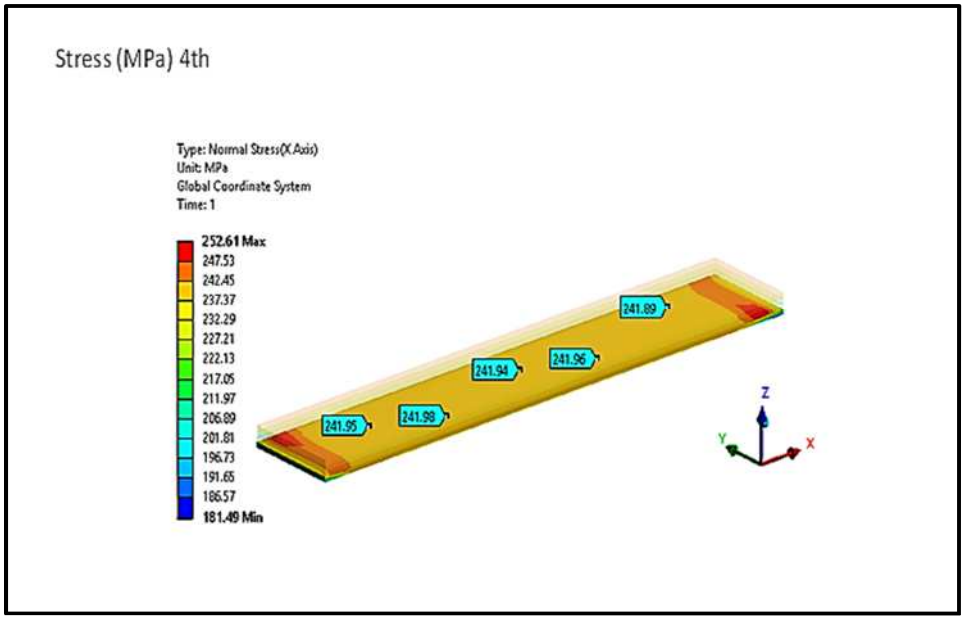

Figure 5.12f: Stress distribution of CC3 in transverse direction on the fourth layer

In Figure 5.13a, deformation 1.1832 mm is observed in Transverse simulation by considering all layers at 0/+60/-60/0 position. In Figure 5.13b, stress behavior is observed as per shown above in Transverse simulation by considering all layers at 0/+60/-60/0 position.

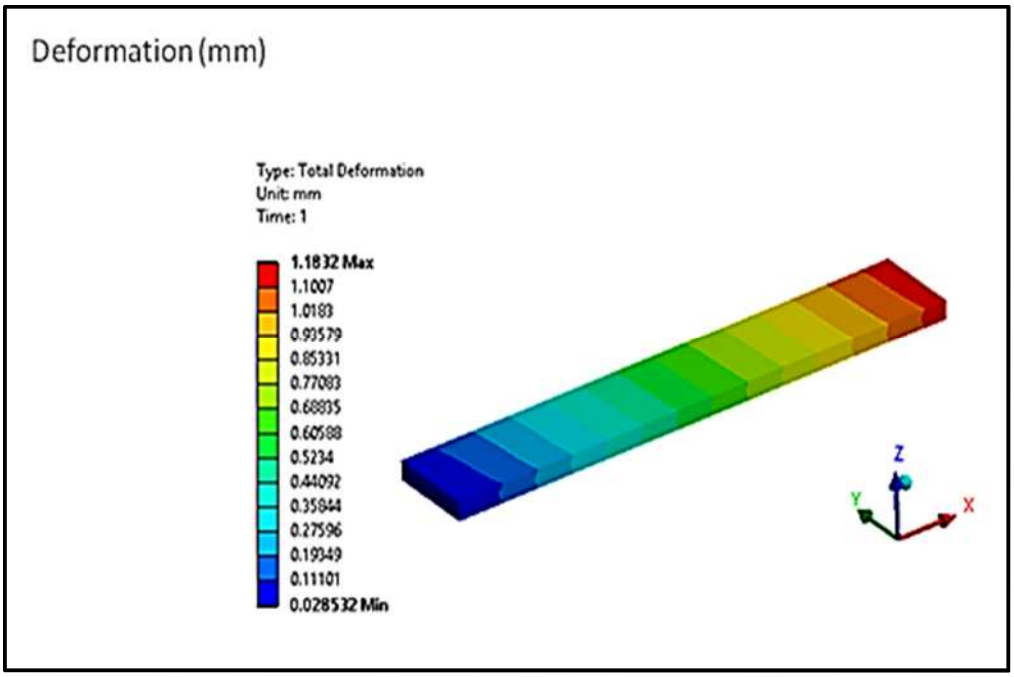

Figure 5.13a: Strain distribution of CC4 in transverse direction

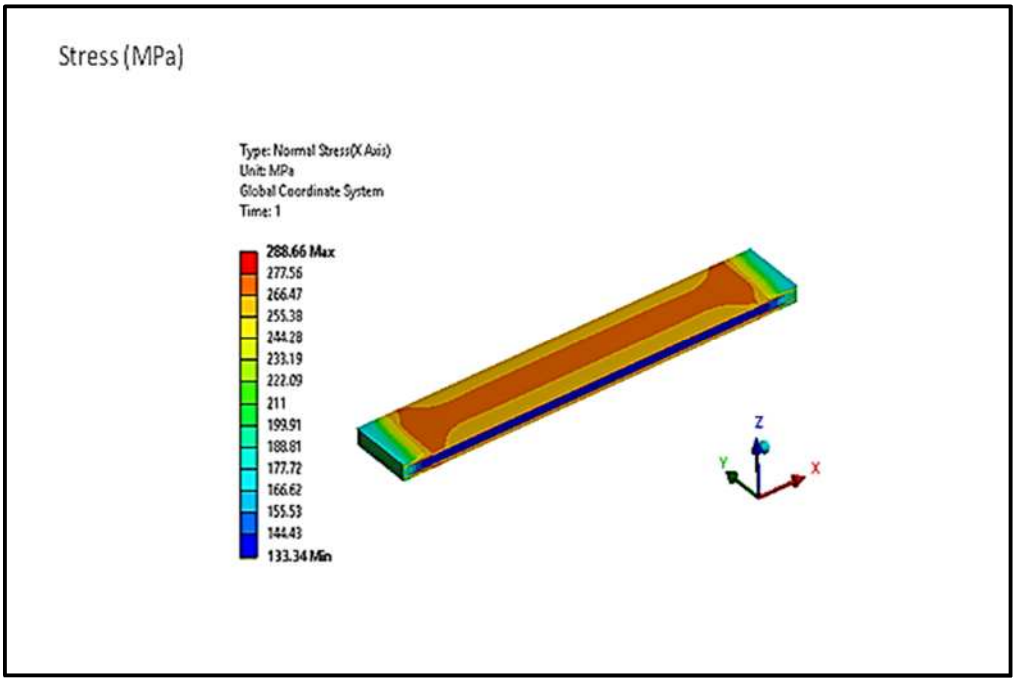

Figure 5.13b: Stress distribution of CC4 in transverse direction

In Figure 5.13c, stress 268.57 MPa is observed as per shown above in Transverse simulation on 1st layer by considering all layers at 0/+60/-60/0 position. In Figure 5.13d, stress 133.34 Mpa is observed as per shown above in Transverse simulation on 2nd layer by considering all layers at 0/+60/-60/0 position.

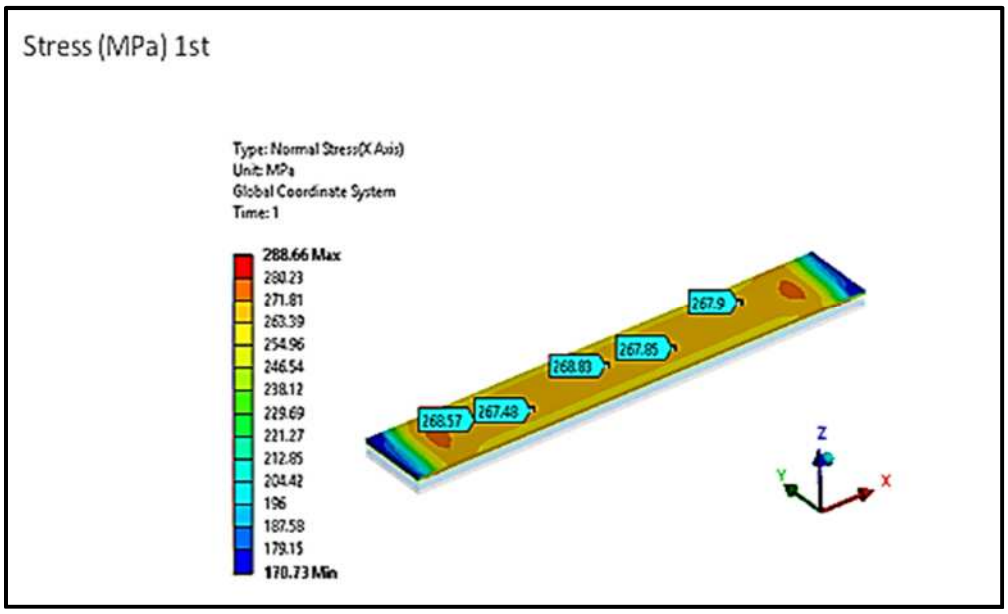

Figure 5.13c: Stress distribution of CC4 in transverse direction on the first layer

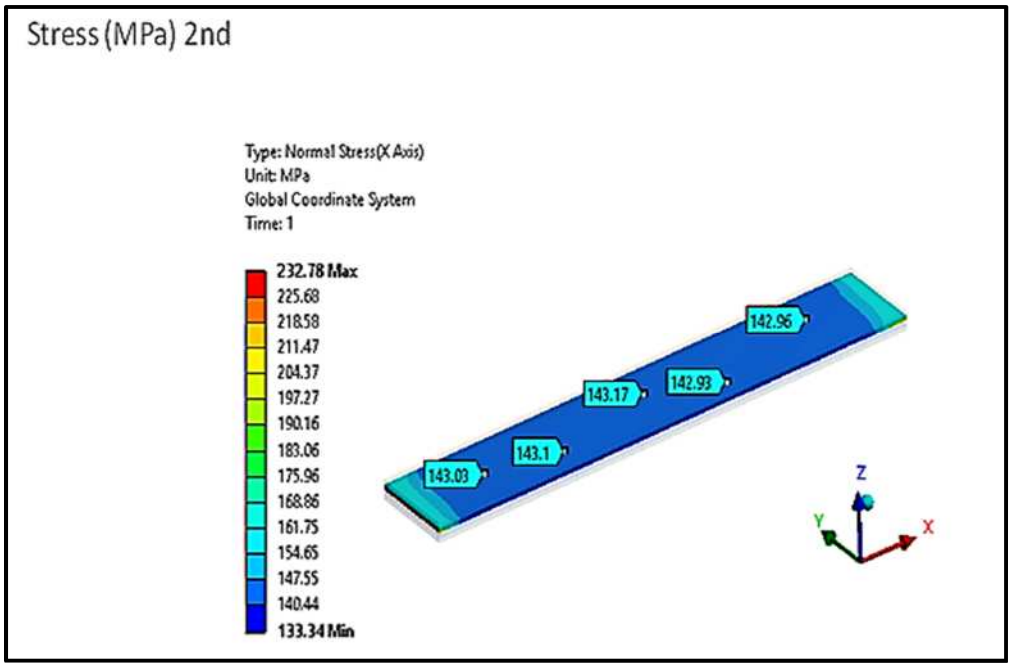

Figure 5.13d: Stress distribution of CC4 in transverse direction on the second layer

In Figure 5.13e, stress 143.93 Mpa is observed as per shown above in Transverse simulation on 3rd layer by considering all layers at 0/+60/-60/0 position. In Figure 5.13f, stress 268.28 MPa is observed as per shown above in Transverse simulation on 4th layer by considering all layers at 0/+60/-60/0 position.

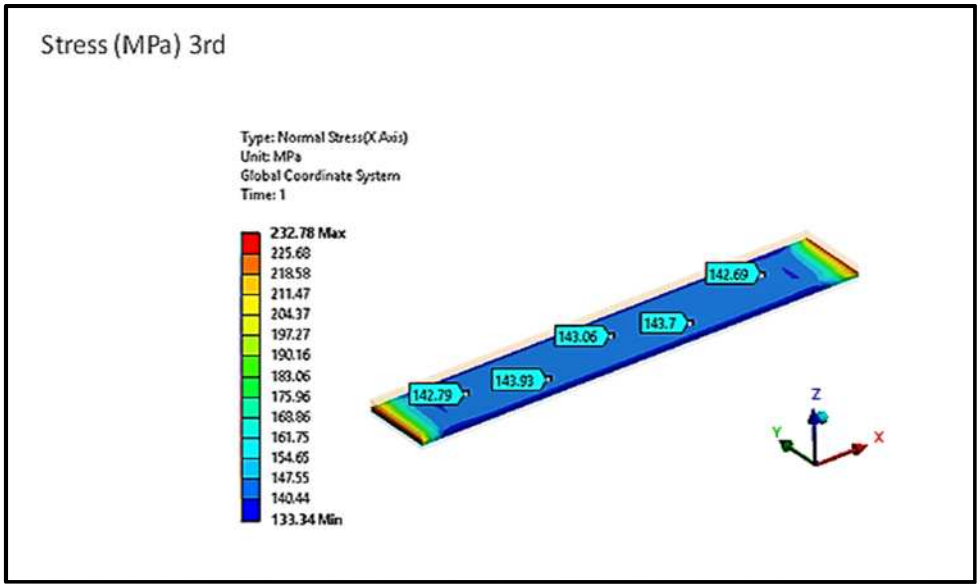

Figure 5.13e: Stress distribution of CC4 in transverse direction on the third layer

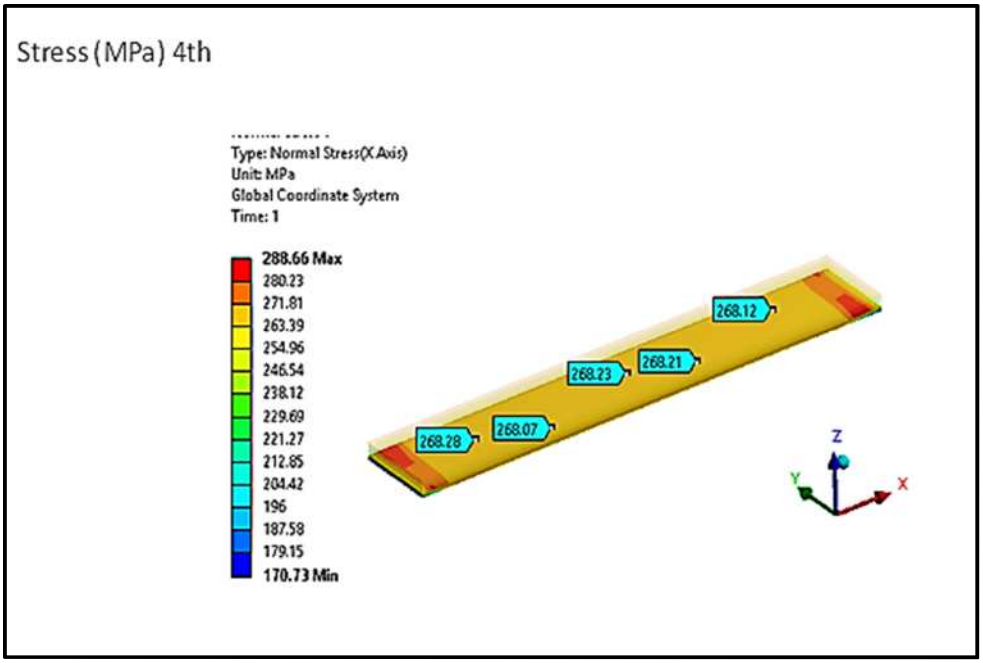

Figure 5.13f: Stress distribution of CC4 in transverse direction on the fourth layer

In Figure 5.14a, deformation 1.29 mm is observed in Transverse simulation by considering all layers at 0/+90/-90/0 position. In Figure 5.14b, stress behavior is observed as per shown above in Transverse simulation by considering all layers at 0/+90/-90/0 position.

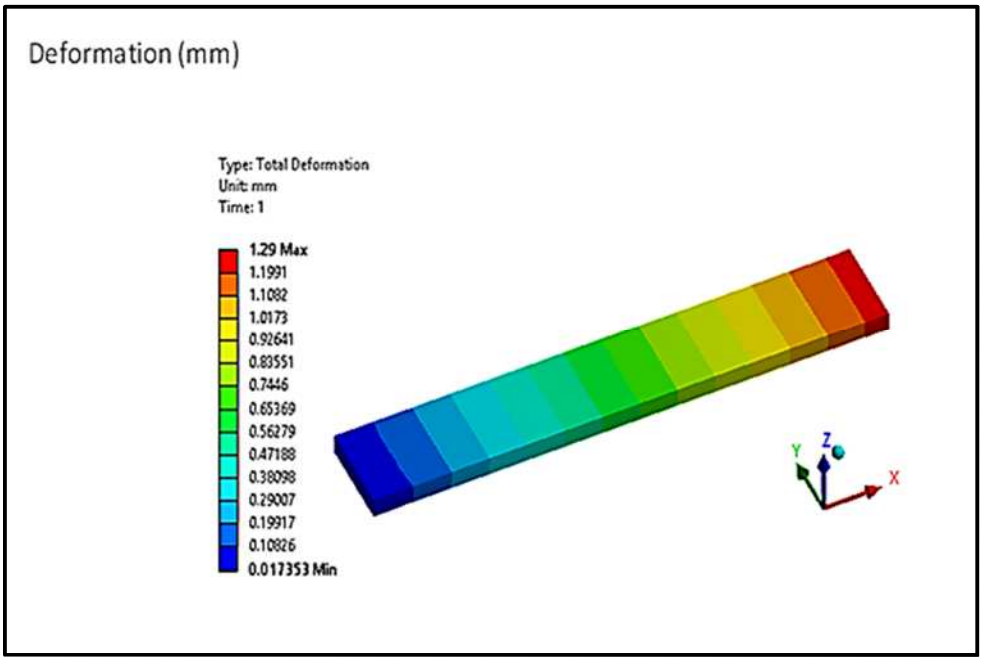

Figure 5.14a: Strain distribution of CC5 in transverse direction

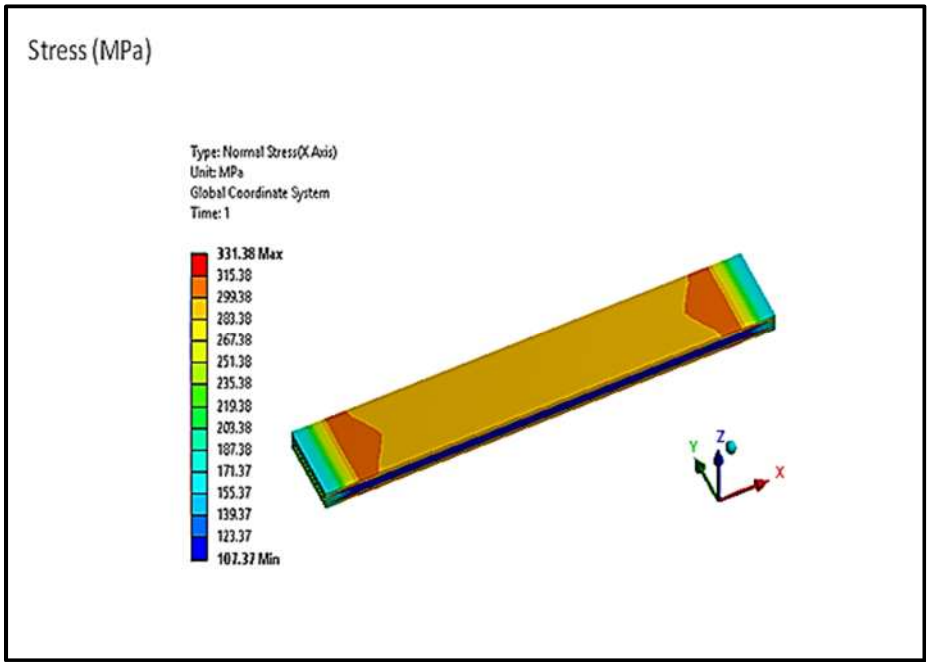

Figure 5.14b: Stress distribution of CC5 in transverse direction

In Figure 5.14c, stress 298.91 Mpa is observed as per shown above in Transverse simulation on 1st layer by considering all layers at 0/+90/-90/0 position. In Figure 5.14d, stress 111.93Mpais observed as per shown above in Transverse simulation on 2nd layer by considering all layers at 0/+90/-90/0 position.

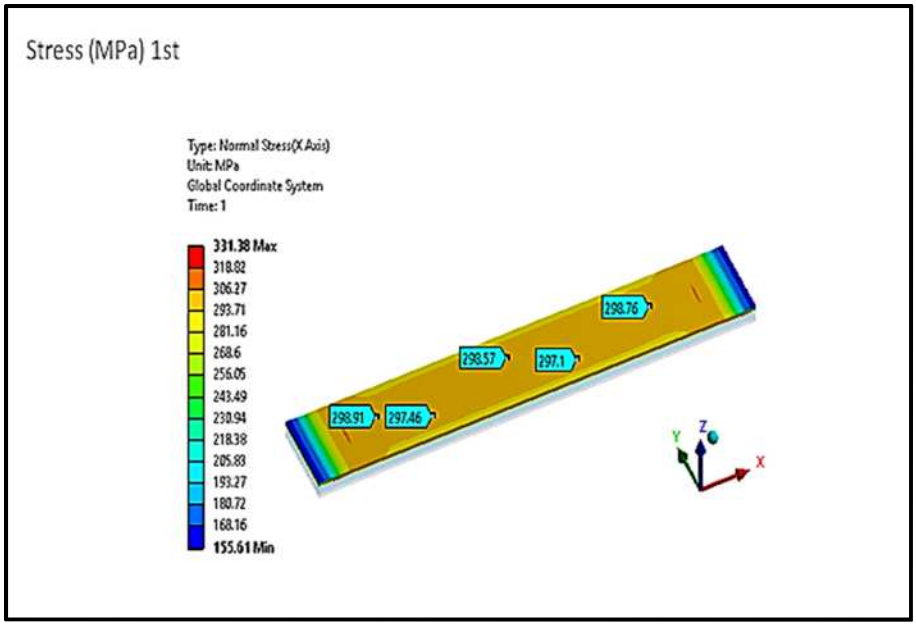

Figure 5.14c: Stress distribution of CC5 in transverse direction on the first layer

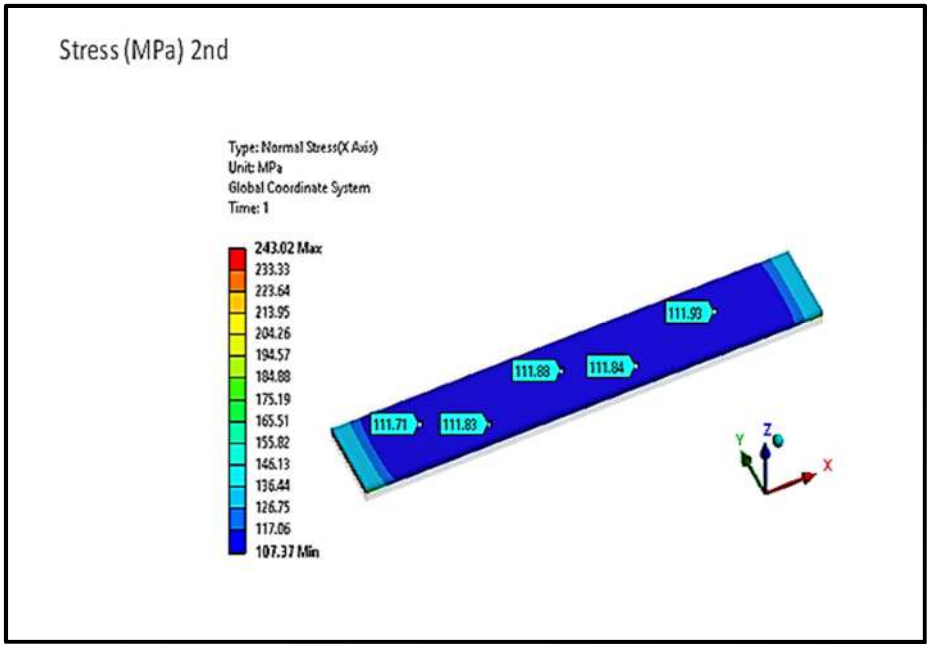

Figure 5.14d: Stress distribution of CC5 in transverse direction on the second layer

In Figure 5.14e, stress 113.2Mpa is observed as per shown above in Transverse simulation on 3rd layer by considering all layers at 0/+90/-90/0 position. In Figure 5.14f, stress 298.89 Mpa is observed as per shown above in Transverse simulation on 4th layer by considering all layers at 0/+90/-90/0 position.

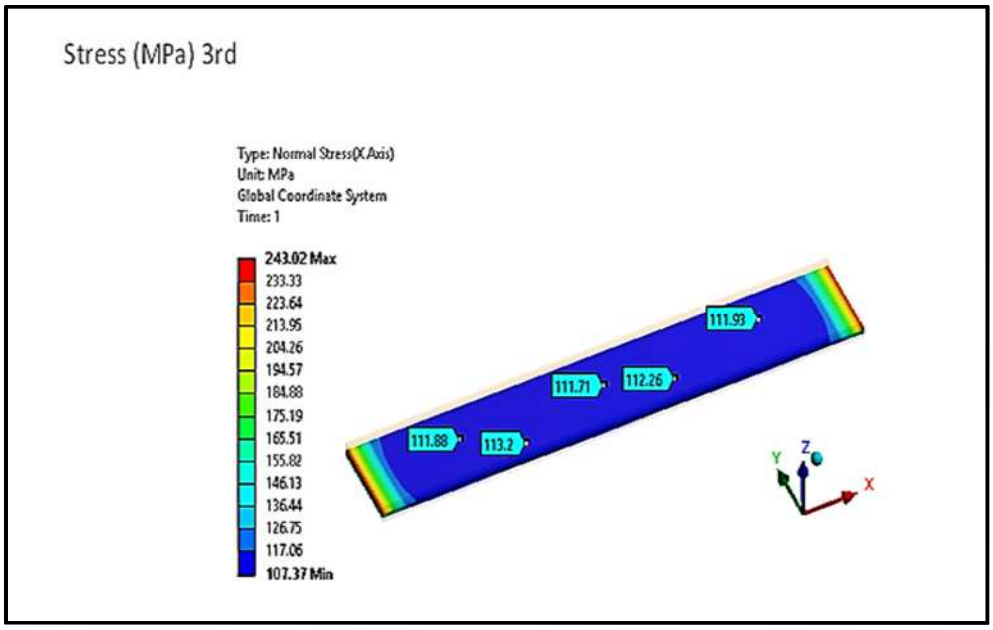

Figure 5.14e: Stress distribution of CC5 in transverse direction on the third layer

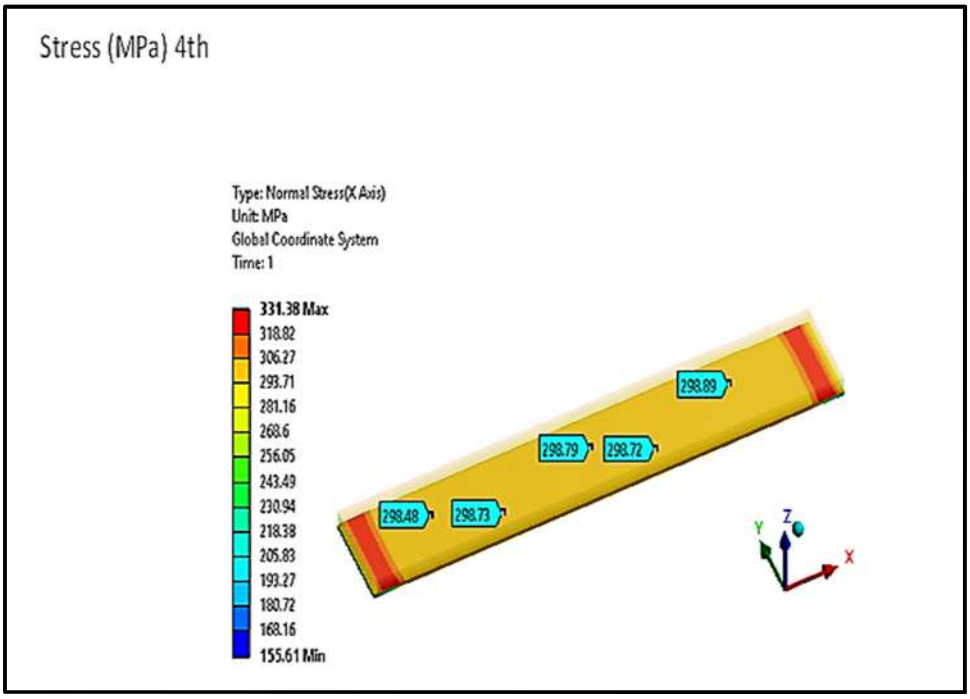

Figure 5.14f: Stress distribution of CC5 in transverse direction on the fourth layer

5.4 Summary and statistical significance

Numerical simulation to discuss the mechanical properties particularly, tensile strength has been done using Finite Element Analysis (FEA) software which uses three dimensional elements with layer capabilities to simulate fibre reinforced composite materials. The analyzed material is a woven carbon fabric($(C_{12K}C_{6K})_p$ with a uniform number of warp and filling threads used for textile polymer textile composite laminate

After simulation in Ansys (post processing) the data had been modelled related to parameters displacement, stress and strain. These data are processed through MS excel to get the comparison between experimental results and modelling results. Table 5.2 depicts the comparison between experimental and modelling results.

Figure 5.15-5.24, shows the comparison of modelling values and experimental values for longitudinal and transverse. The fabric orientation considered is (0/0/0/0, 0/±30/0, 0/±45/0, 0/±60/0 and 0/±90/0).

In Regression analysis R^2 is a measure in statistics that will give information about how best the goodness of fit of a model. It also gives information about how well the regression predictions approximate the real data points. An R^2 of 1 indicates that the regression predictions perfectly fit the data.

We have done the comparison of modelling values and experimental values for longitudinal and transverse. The fabric orientation considered is (0/0/0/0, 0/±30/0, 0/±45/0, 0/±60/0 and 0/±90/0).

It is seen from the Figures 5.15-5.24 data that had been fitted are linear. It is true also as the R^2 is closer to 1 or 1. Therefore, in our case linearity is the best fitting. Experience on this analysis says that the other kind of data fitting like quadratic, exponential and logarithmic does not work because the R^2 value is not closer to 1 or 1.

Table 5.2: Comparison of experimental and modeling results

Strain	Stress	Strain	Stress	Strain	Stress	Strain	Stress	Strain	Stress	Strain	Stress	Strain	Stress	Strain	Stress	Strain	Stress	Strain	Stress
%	Mpa	%	Mpa	%	Mpa	%	Mpa	%	Mpa	%	Mpa	%	Mpa	%	Mpa	%	Mpa	%	Mpa
CC1				CC2				CC3				CC4				CC5			
EXP		*MOD*		*EXP*		*MOD*		*EXP*		*MOD*		*EXP*		*MOD*		*EXP*		*MOD*	
LONGITUDINAL																			
0	0	0	0	0	0	0	0	0	0	0	0	0	0	0	0	0	0	0	0
0.6	27.09	0.91575	50	0.6	38.71	0.79872	50	0.62	45.53	0.64749	50	0.6	48.85	0.56535	50	0.59	47.38	0.51073	50
0.9	42.42	1.8315	100	0.9	53.36	1.59744	100	1.2	69.5	1.29497	100	0.89	64.95	1.13069	100	0.84	69.99	1.02145	100
1.8	89.19	2.74725	150	1.3	72.66	2.39617	150	1.8	98.7	1.94246	150	1.27	93.07	1.69604	150	1.73	132.11	1.53218	150
2.52	136.12	3.75458	205	1.82	103.32	3.27476	205	2.4	130.37	2.65469	205	1.78	128.35	2.31792	205	2.53	196.85	2.09397	205
3.45	191.68			2.53	142.26			3	158.32			2.87	184.31			3.27	266.43		
				3.92	202.43			3.42	175.7			4.38	239.45			3.52	293.72		
																4.4	372.52		
																6.26	456.73		
TRANSVERSE																			
EXP		*MOD*		*EXP*		*MOD*		*EXP*		*MOD*		*EXP*		*MOD*		*EXP*		*MOD*	
0	0	0	0	0	0	0	0	0	0	0	0	0	0	0	0	0	0	0	0
0.89	116.61	0.35411	50	0.06	8.95	0.59347	50	0.03	3.81	0.55615	50	0.88	67.17	0.53055	50	1.82	180.65	0.51073	50
2.59	352.81	0.70822	100	1.8	130.15	1.18694	100	1.8	92.98	1.1123	100	2.55	187	1.06109	100	2.56	252.27	1.02145	100
4.26	634.88	1.06232	150	3.4	254.19	1.78042	150	3.41	193.56	1.66845	150	4.2	300.62	1.59164	150	3.39	339.01	1.53218	150
5.94	894.04	1.45184	205	4.8	354.81	2.43323	205	4.21	251.47	2.28021	205	4.77	335.28	2.17524	205	4.2	417.79	2.09397	205
6.27	980.06			5.33	401.01			5.76	352.68			5.1	365.78			4.29	437		

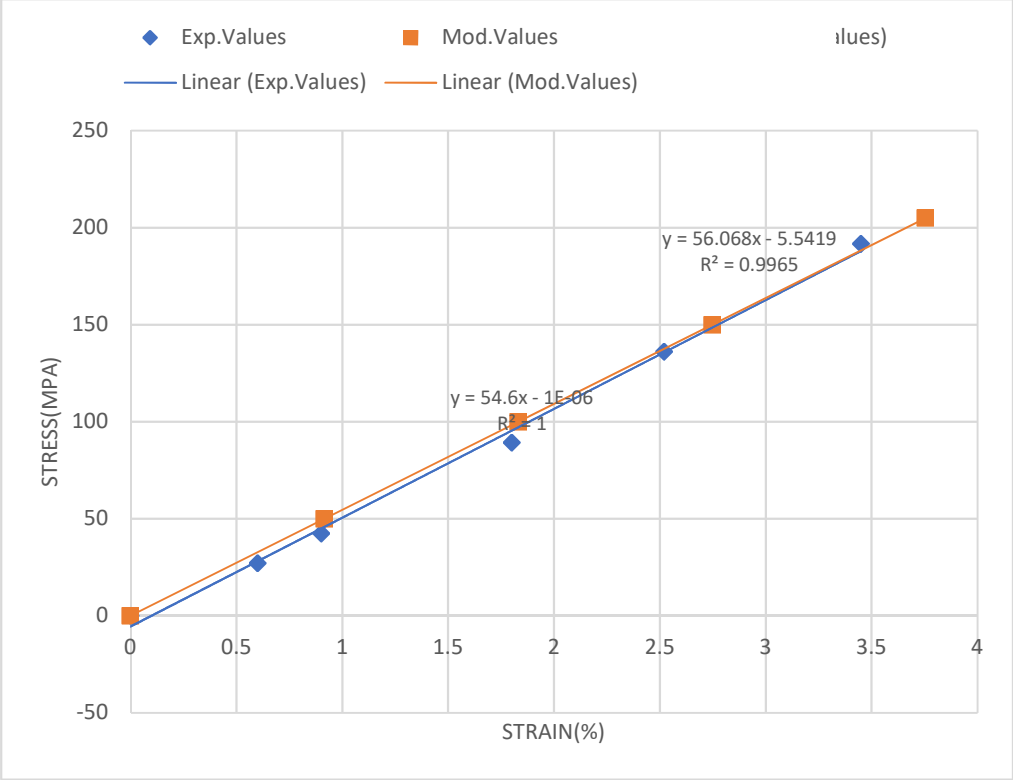

Figure 5.15: Comparison of Modelling Values and Experimental values for longitudinal case if the fabric orientation is 0/0/0/0

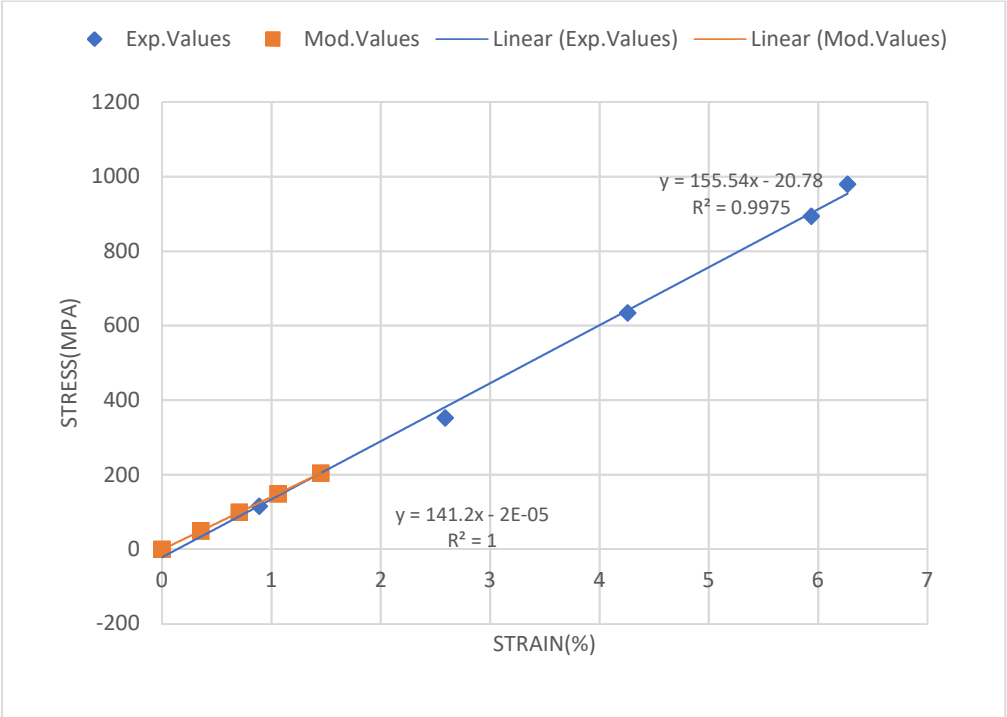

Figure 5.16: Comparison of Modelling Values and Experimental values for Transverse case if the fabric orientation is 0/0/0/0

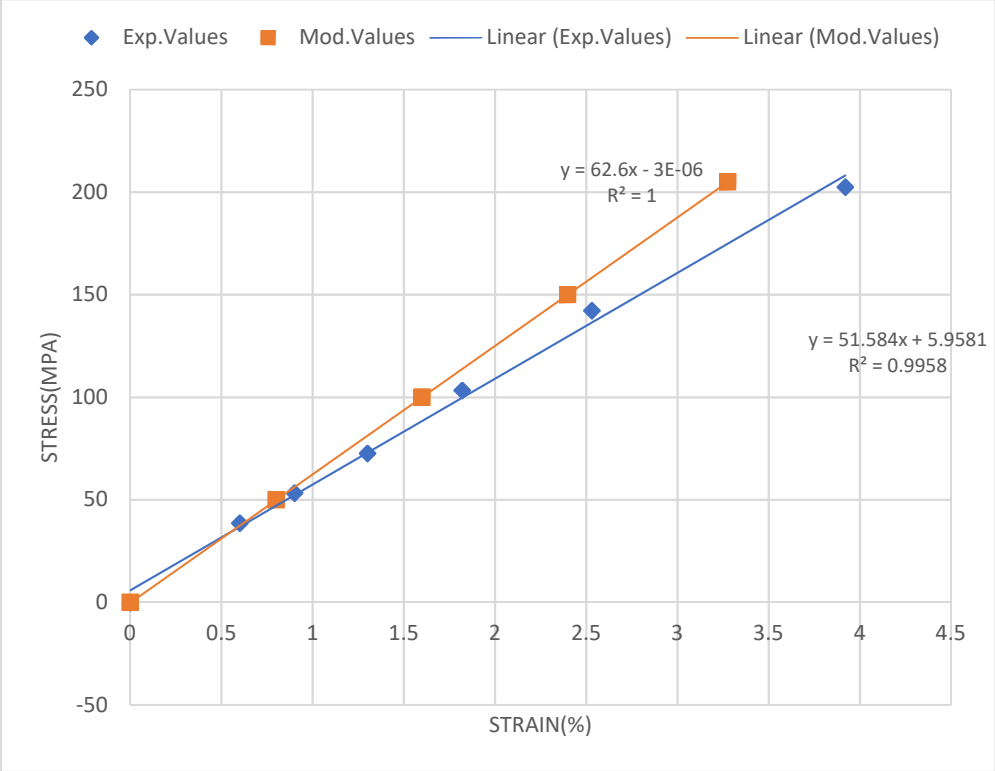

Figure 5.17: Comparison of Modelling Values and Experimental values for longitudinal case if the fabric orientation is 0/30/30/0

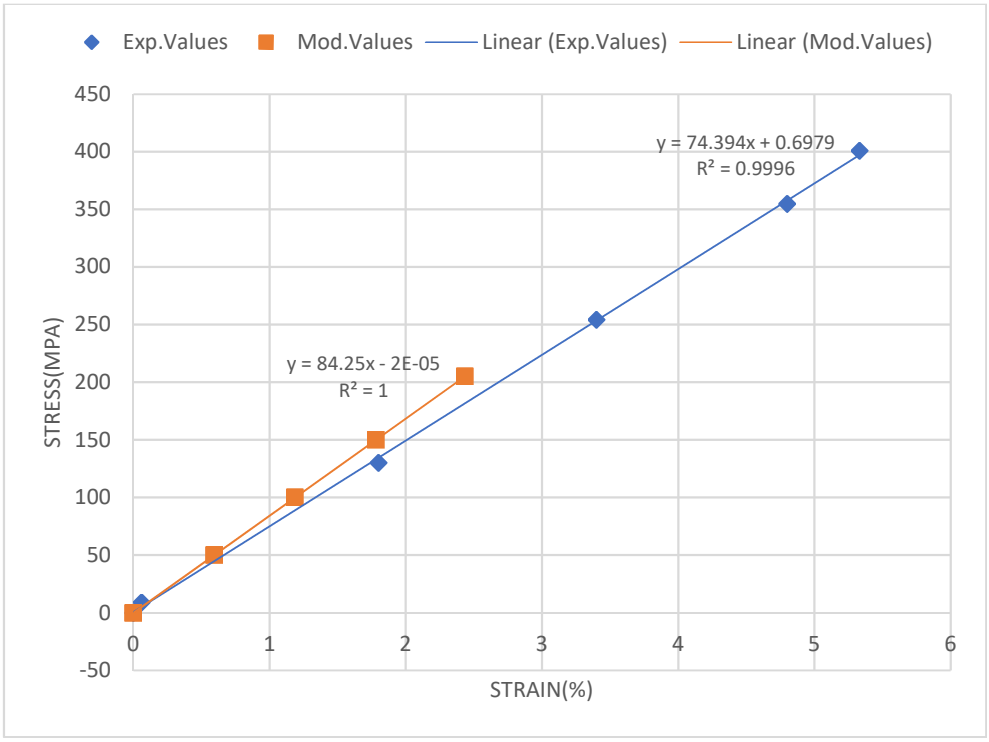

Figure 5.18: Comparison of Modelling Values and Experimental values for Transverse case if the fabric orientation is 0/30/30/0

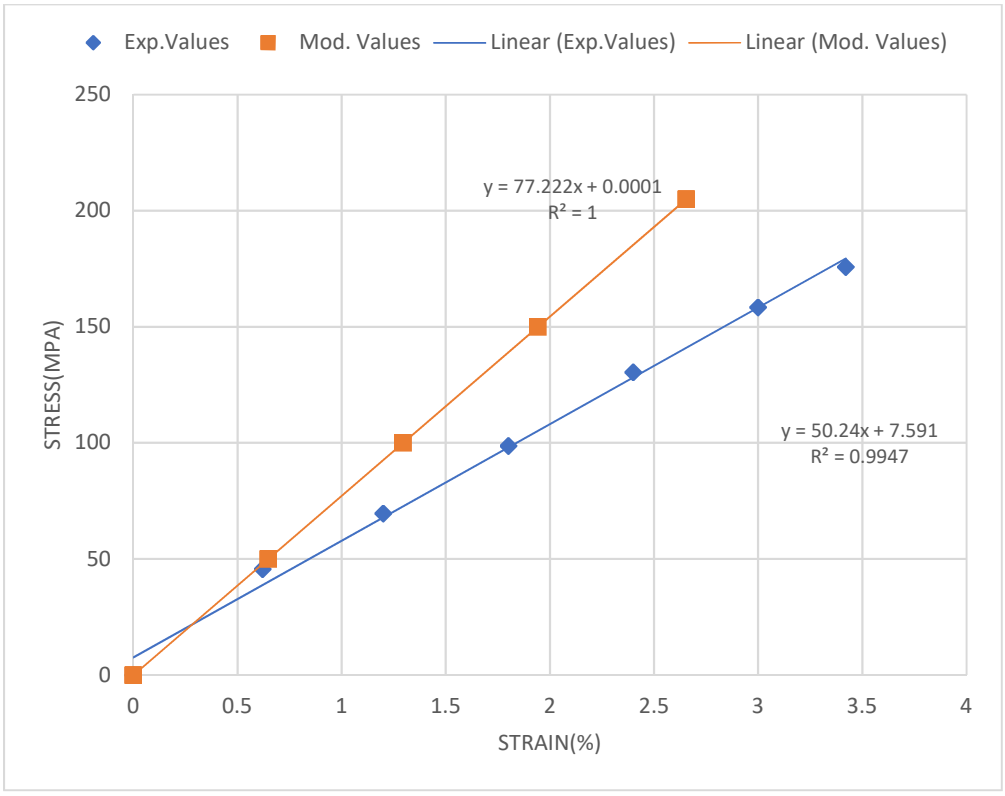

Figure 5.19: Comparison of Modelling Values and Experimental values for longitudinal case if the fabric orientation is 0/45/45/0

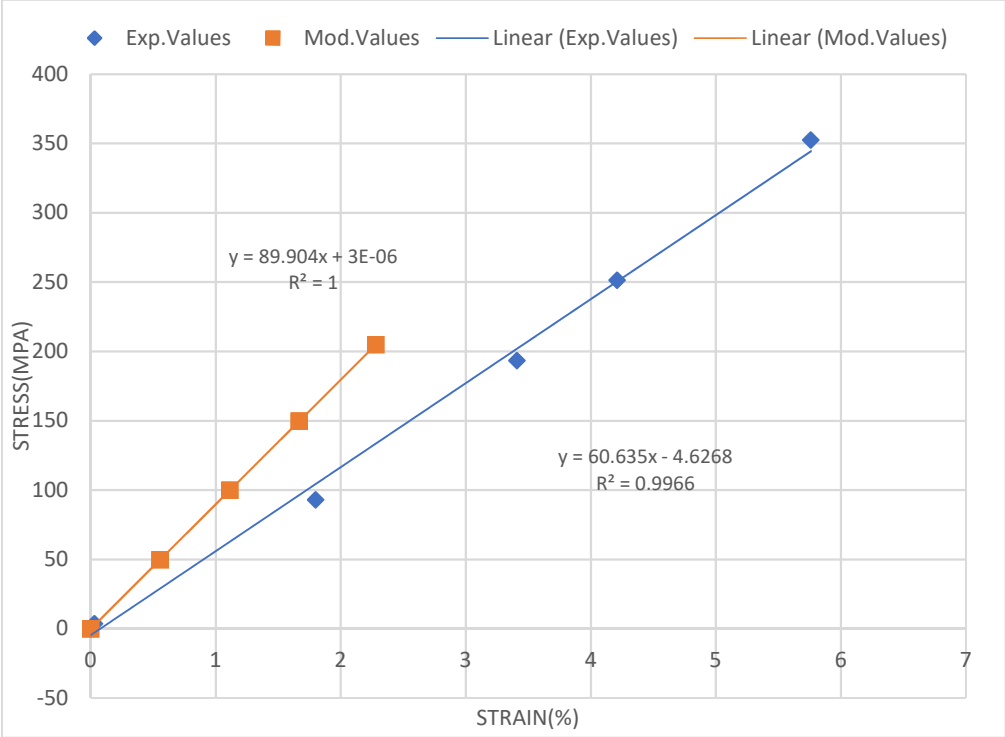

Figure 5.20: Comparison of Modelling Values and Experimental values for Transverse case if the fabric orientation is 0/45/45/0

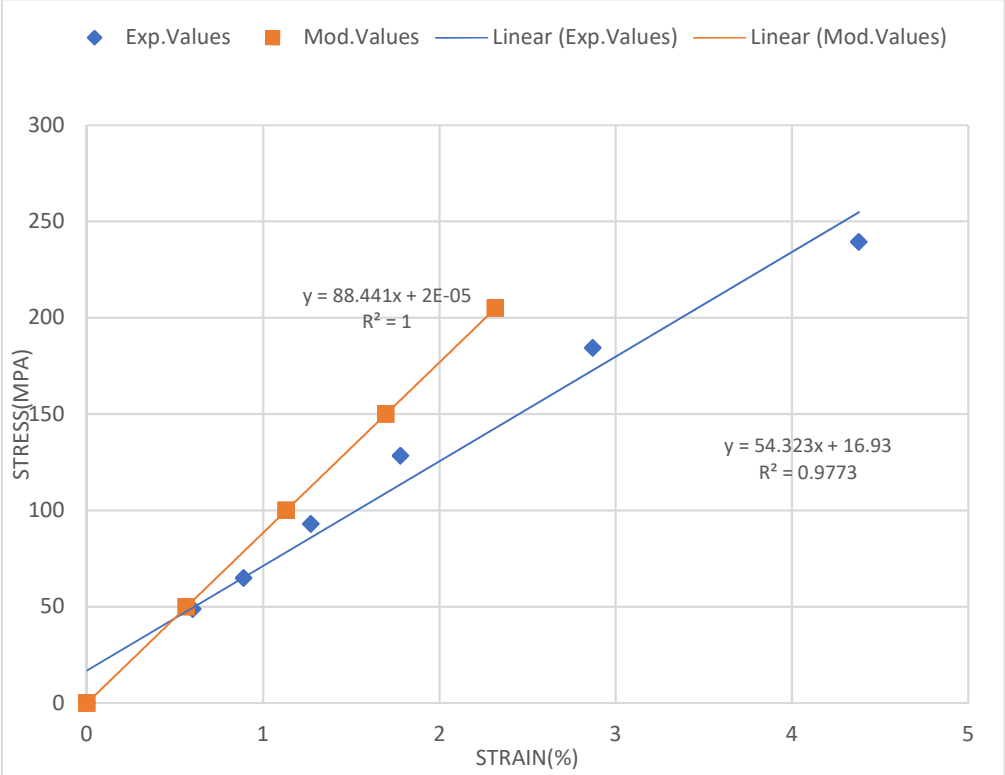

Figure 5.21: Comparison of Modelling Values and Experimental values for longitudinal case if the fabric orientation is 0/60/60/0

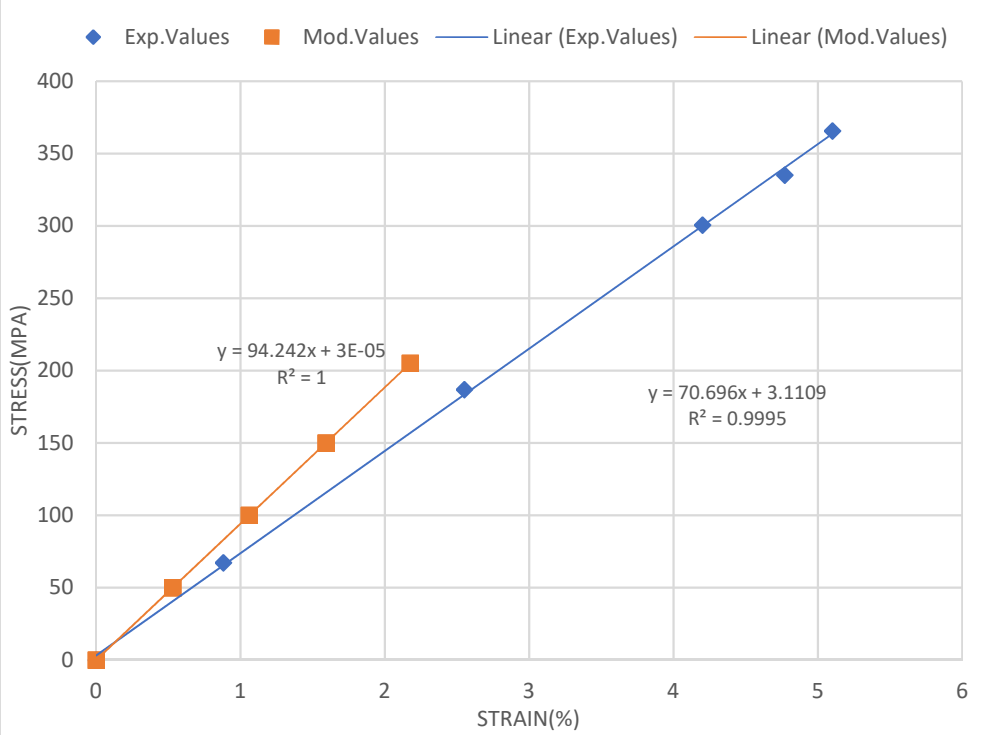

Figure 5.22: Comparison of Modelling Values and Experimental values for Transverse case if the fabric orientation is 0/60/60/0

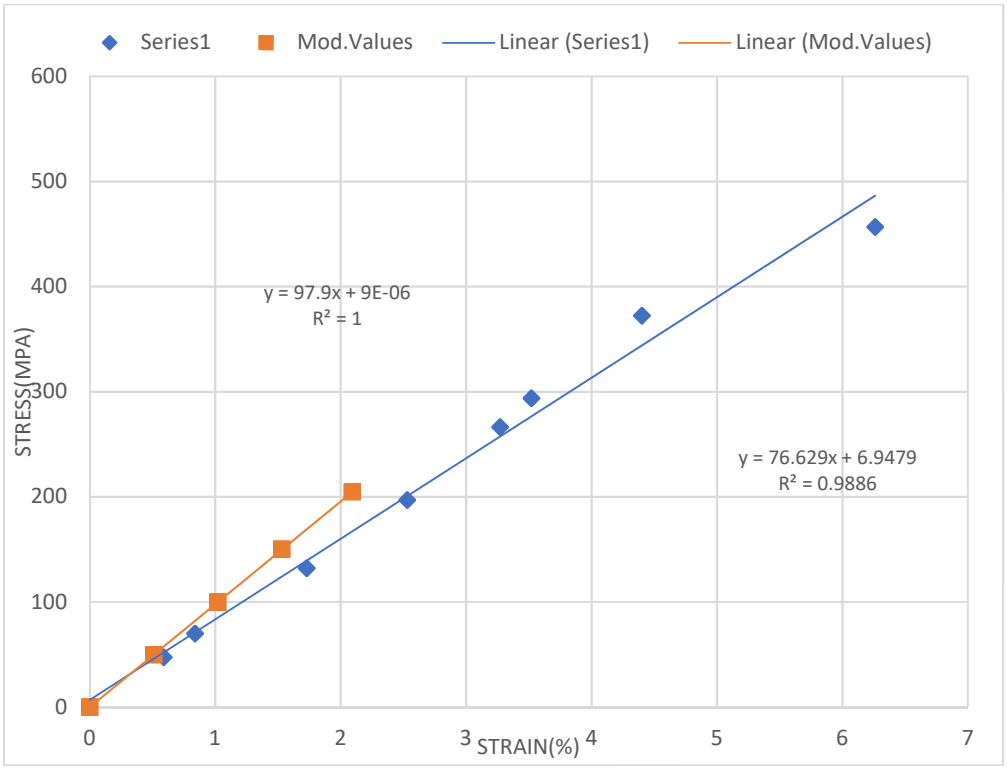

Figure 5.23: Comparison of Modelling Values and Experimental values for longitudinal case if the fabric orientation is 0/90/90/0

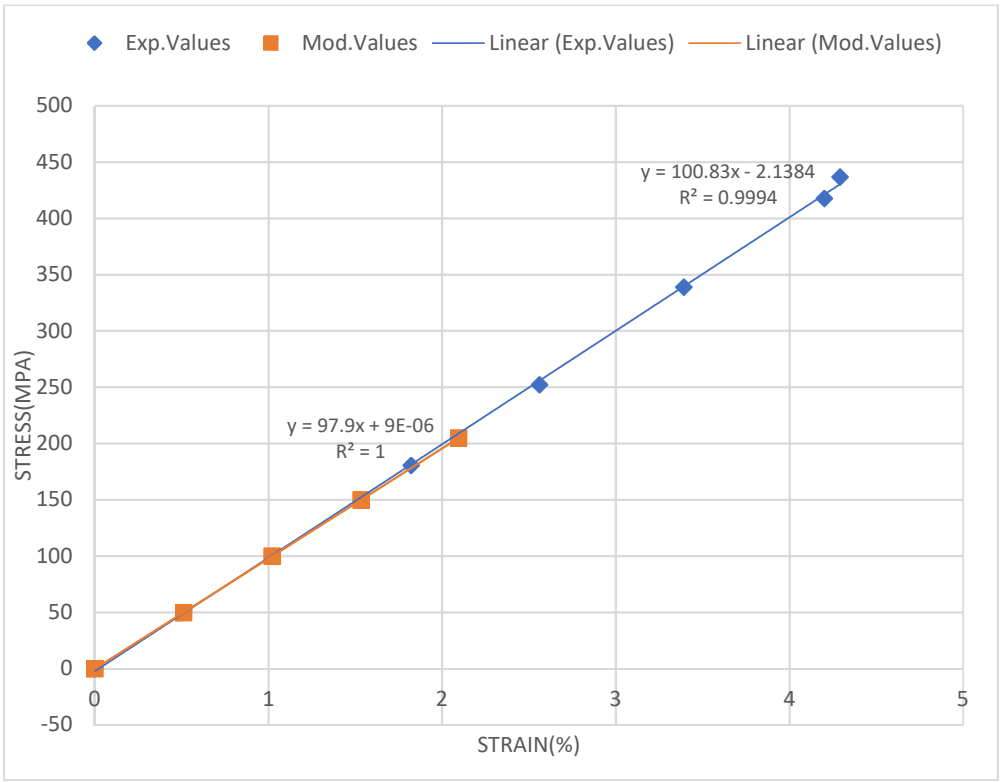

Figure 5.24: Comparison of Modelling Values and Experimental values for Transverse case if the fabric orientation is 0/90/90/0

5.5 Conclusion

FEM techniques require first decomposition of textile composites and which can be visualized as assemblages of representative volume elements interconnected at discrete numbers of nodal points.

Now, discretization or decomposition of the domain into finite elements was done using software Solid works. Here, the finite element has been considered as hexahedral mesh. Equations for each element have been developed. After applying boundary conditions, initial conditions and loading, the global stiffness matrix has been constructed. Later on, a set of linear or nonlinear algebraic equations have been solved simultaneously to obtain nodal displacement results. Using displacements, the strain value was found. Using Poison's ratio in Ansys stress had been evaluated.

It is also observed that experimental and modelling results are matching within ±10% variation for longitudinal and transverse axis for zero degree. There is no contact stiffness considered in analysis between layers. Experimental testing is based on axial behavior only and it is performed for checking combine behavior for all four layers to find out axial strength only. There is not a scope to test bonding behavior of layers to find out layers shear behavior and its contact stiffness. The linearity is best fitted to the data points as the R^2 value is closer to 1 or 1.

In Simulation, contact stiffness of layers are considered infinite i.e. RBEs elements are considered between layer to layer contact. So, for the axial testing, graphs variation is high by increasing angles and by increasing loads. It can be concluded that experimental and simulated results are matching for all angles at small value of loads.

Experimental and simulation data are matching up to a certain amount of load application. By increasing load application, shear will come into picture which plays a role to increase deformation more and it breaks the linearity between load v/s deformation. So, the difference/error is high at more load values.

It is important to observe that the FEM evaluation can be done for any composite (at every point) having multilayers and therefore no need to go for experimental testing. The FEM simulation gives the strength and stress distribution at entire fabric composite which cannot be expected from experimental simulation. A higher thickness bonding material can be attempted to achieve a good strength of material.